CEC/ICMC 2013, Cryogenic Engineering Conference and International Cryogenic Materials Conference, Anchorage, June 17-21, 2013

Selection and properties of structural materials for cryogenic applications

Stefano Sgobba
EN-MME-MM
CERN

Outline

- The construction and operation of LHC and its experiments: an almost unique selection ground and testing bench for structural materials
- LHC, examples of successful innovative solutions
  - *The LHC beam screen*
  - *The 2500 near net shaped HIPed PM end covers*
- LHC experiments, the CMS example
  - *Reinforcement of the CMS Al-stabilized conductor produced in continuous 2.5 km lengths*
  - *Al-alloy end flanges of the 6.8 m diameter external cylinder of the 4 T superconducting solenoid*
- Ongoing developments
  - *Innovative materials for conductors of future particle experiments*
  - *Selection and characterization of structural materials for fusion magnets*
- Conclusion
  - *Materials to be identified together with a suitable manufacturing process at an early stage of a project*


F
S
C
A

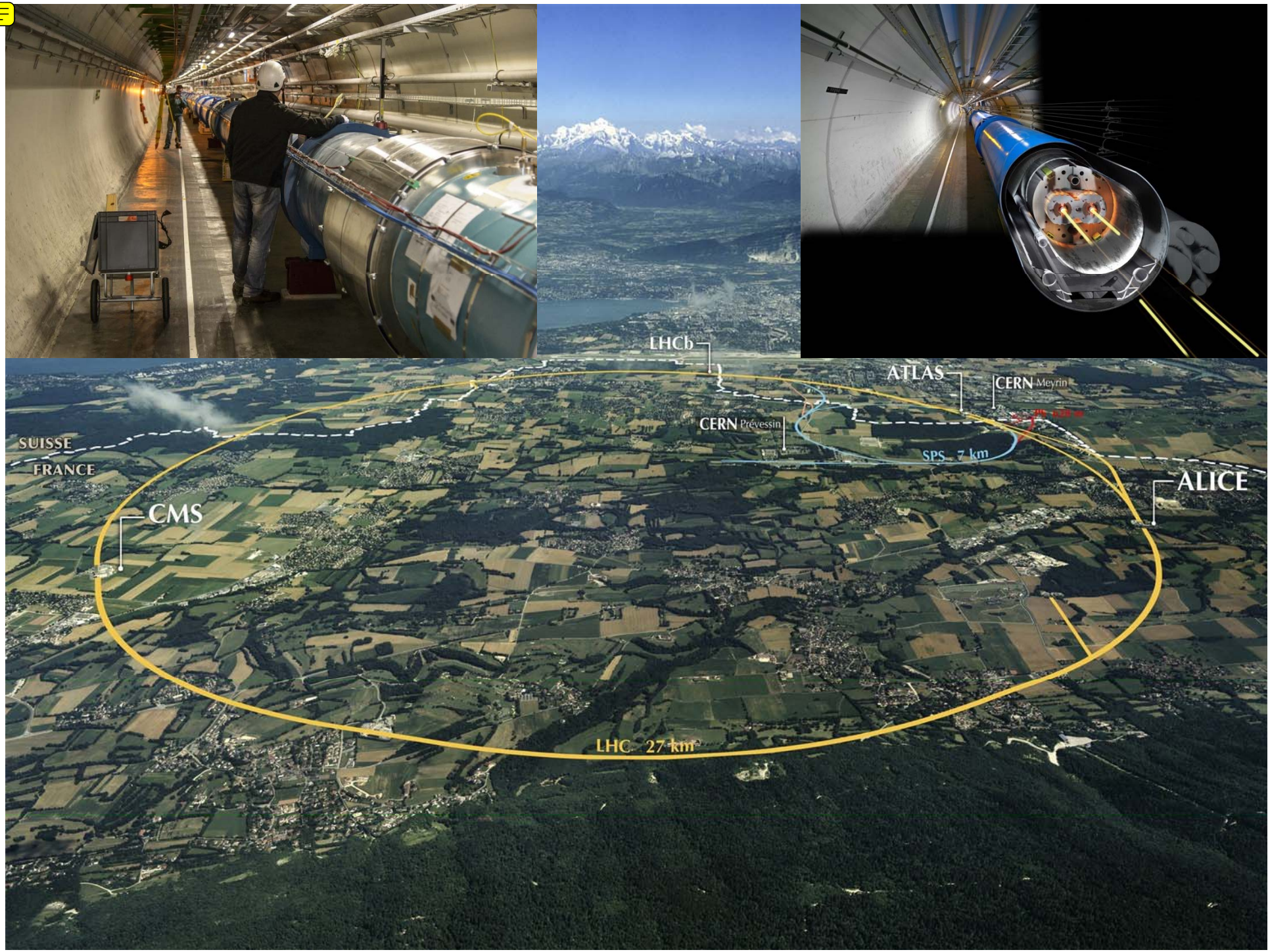
LHCb
ATLAS
CERN Meyrin
CERN Prévessin
SPS 7 km
SUISSE
FRANCE
CMS
ALICE
LHC 27 km

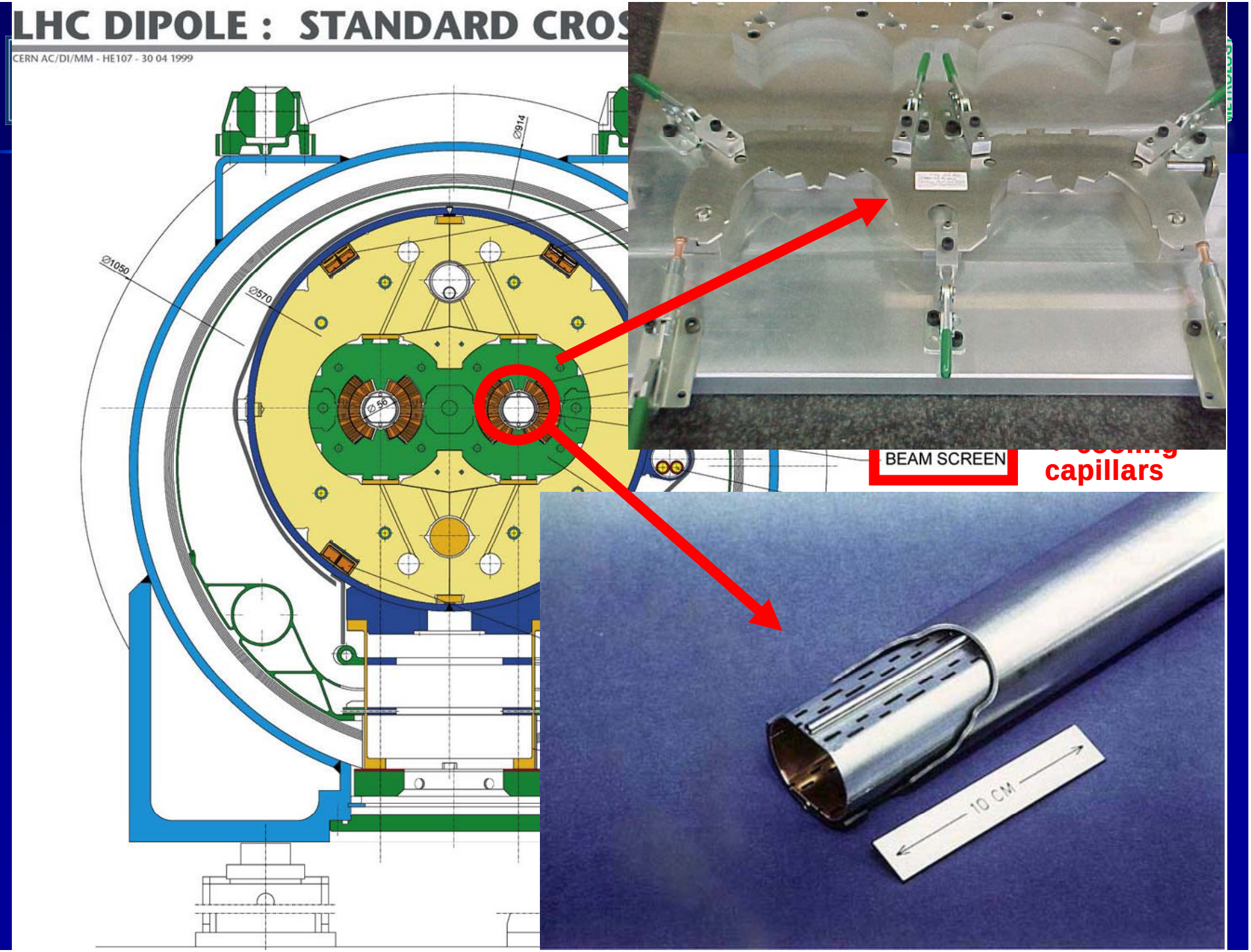
LHC DIPOLE : STANDARD CROS
CERN AC/DI/MM - HE107 - 30 04 1999
∅914
∅1050
∅570
∅56
BEAM SCREEN
capillars
10 CM

LHC DIPOLE : STANDARD CROSS-SECTION

CERN AC/DI/MM - HE107 - 30 04 1999

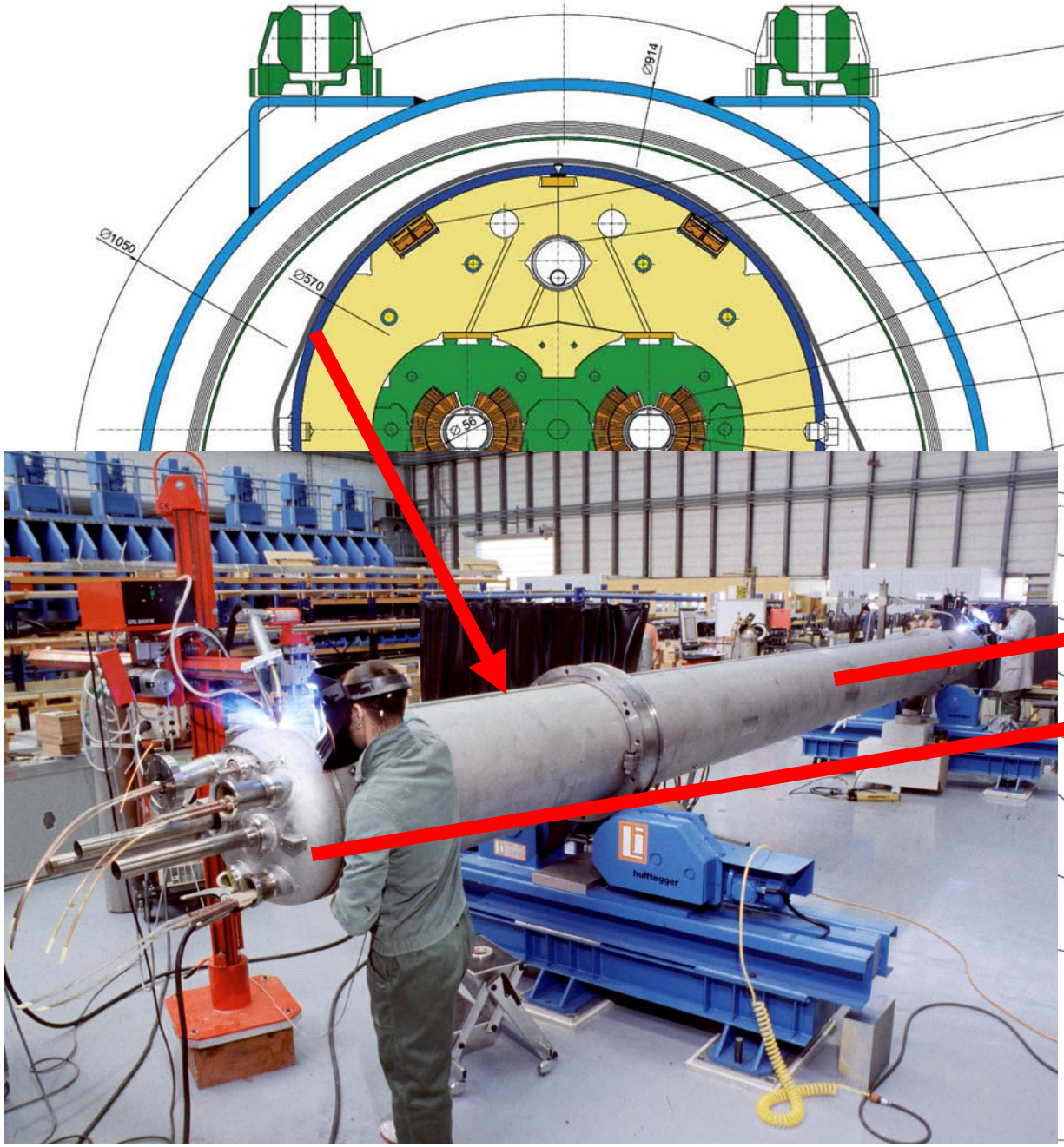

ALIGNMENT TARGET
MAIN QUADRIPOLE BUS-BARS
HEAT EXCHANGER PIPE
SUPERINSULATION
SUPERCONDUCTING COILS
BEAM PIPE
VACUUM VESSEL
BEAM SCREEN
AUXILIARY BUS-BARS
SHRINKING CYLINDER / HE I-VESSEL
THERMAL SH + end covers
NON-MAGNETIC COLLARS
IRON YOKE (COLD MASS, 1.9K)
DIPOLE BUS-BARS
SUPPORT POST

LHC DIPOLE : STANDARD CROSS-SECTION

CERN AC/DI/MM - HE107 - 30 04 1999

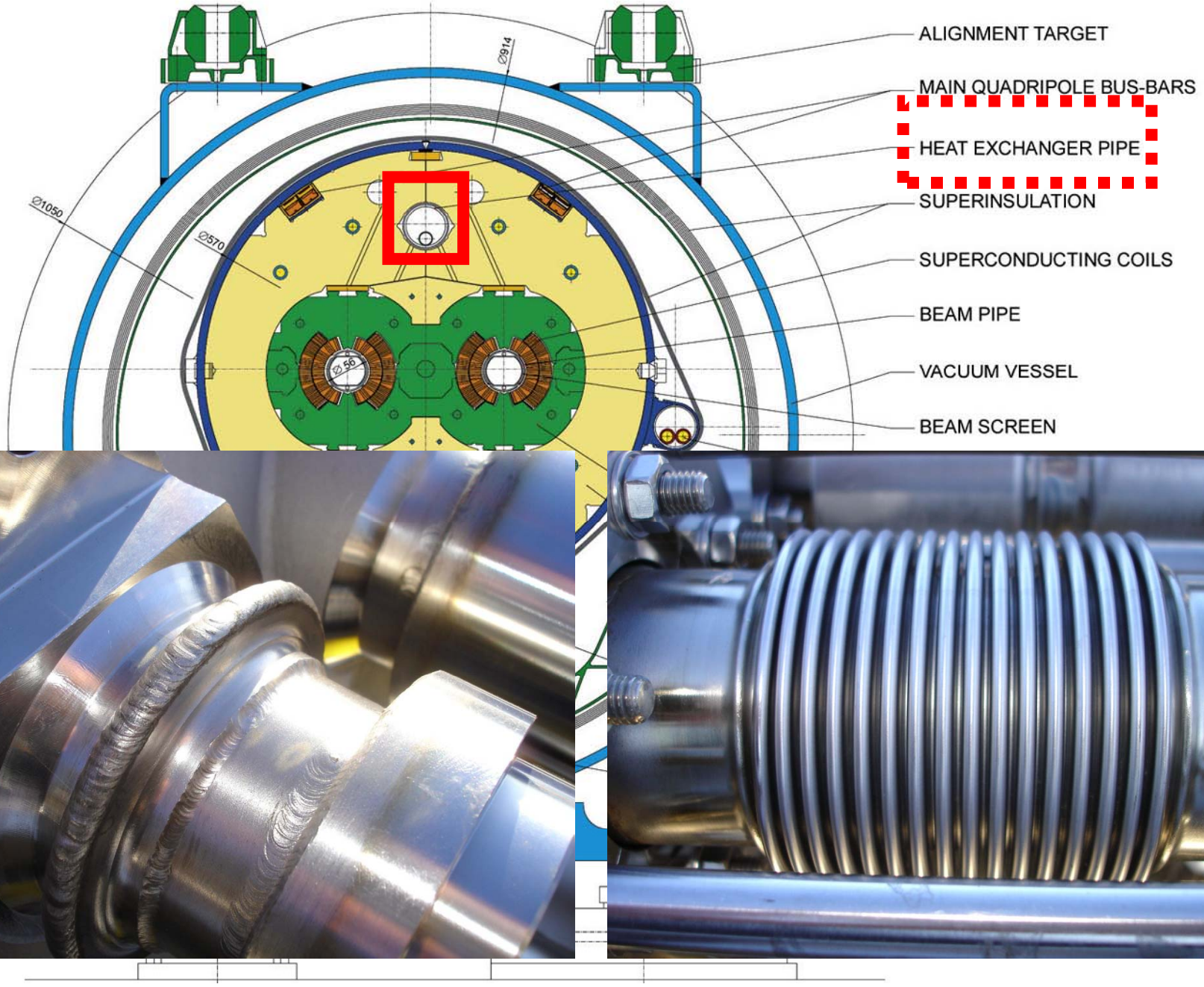

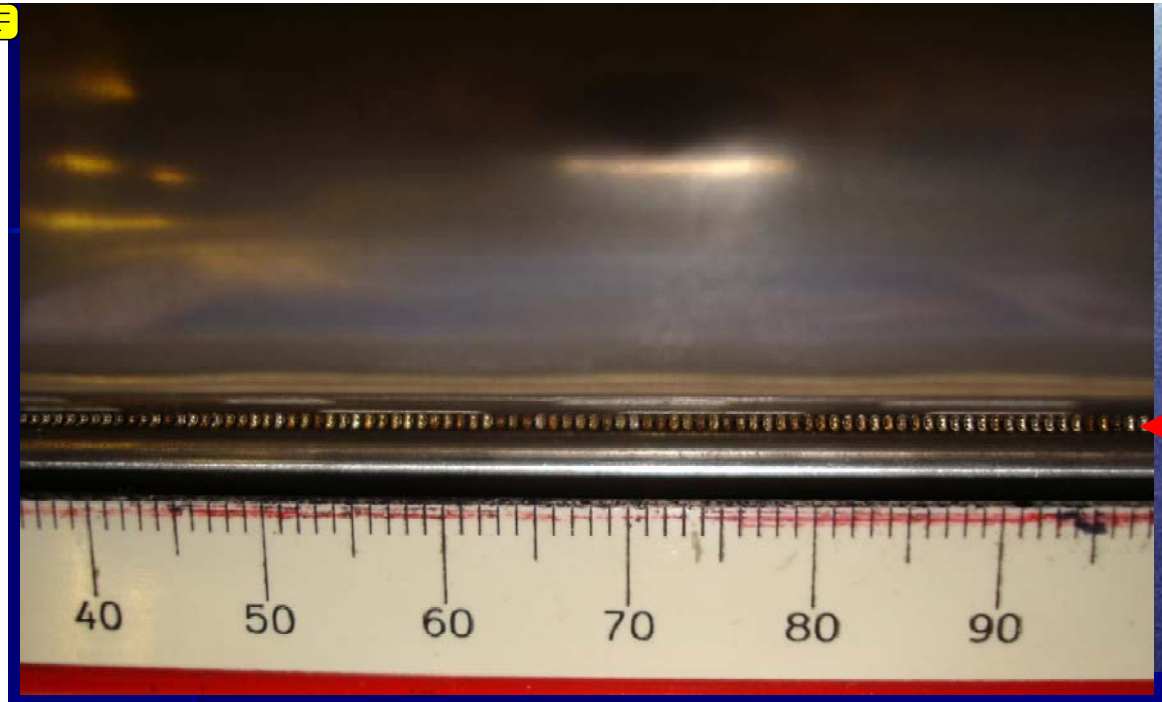

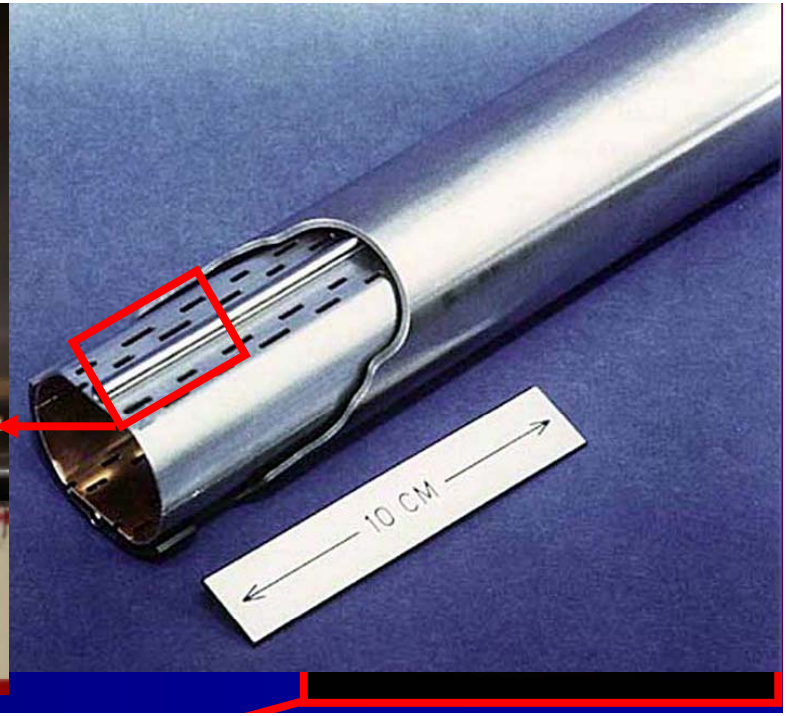

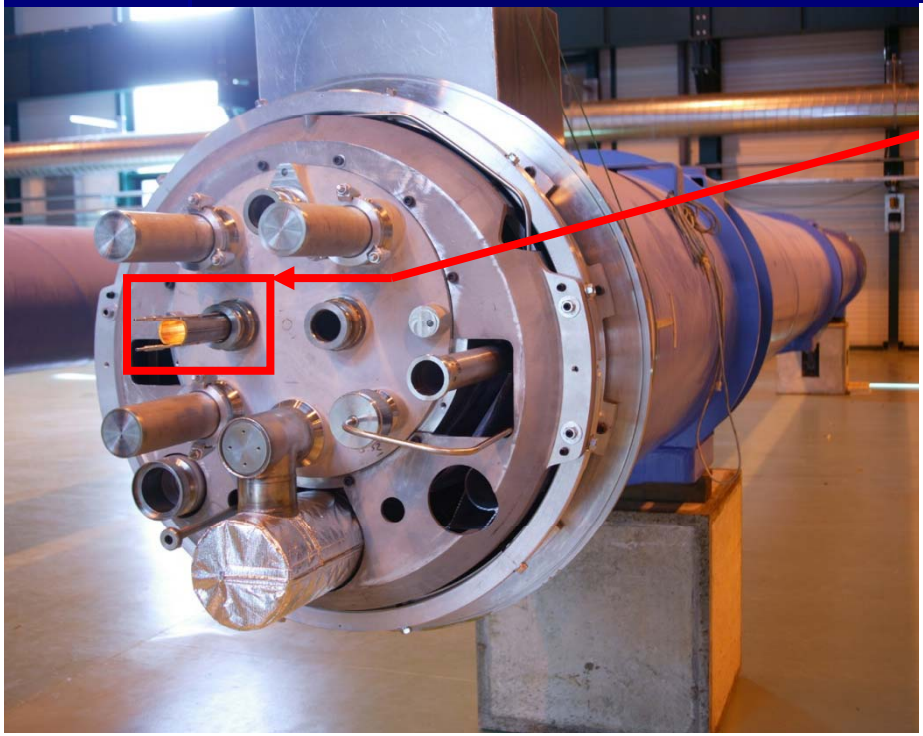

Development of a new stainless steel for the LHC beam screen and the cooling capillaries

Challenging scope:

- Magnetic susceptibility $\leq 5 \cdot 10^{-3}$ at operating T in weld and parent material
- Fully stable
- Millions of laser welding points fully leak tight
- Absence of hot cracking
- High strength and toughness (> 200 J)
- Thermal contraction not far from 316LN
- Corrosion behaviour ≈ 304L, 316LN
- Affordable price (several tens of km…)

Examples of innovative solutions: LHC beam screen

Compared magnetic susceptibility of different austenitic SS and their laser weldments

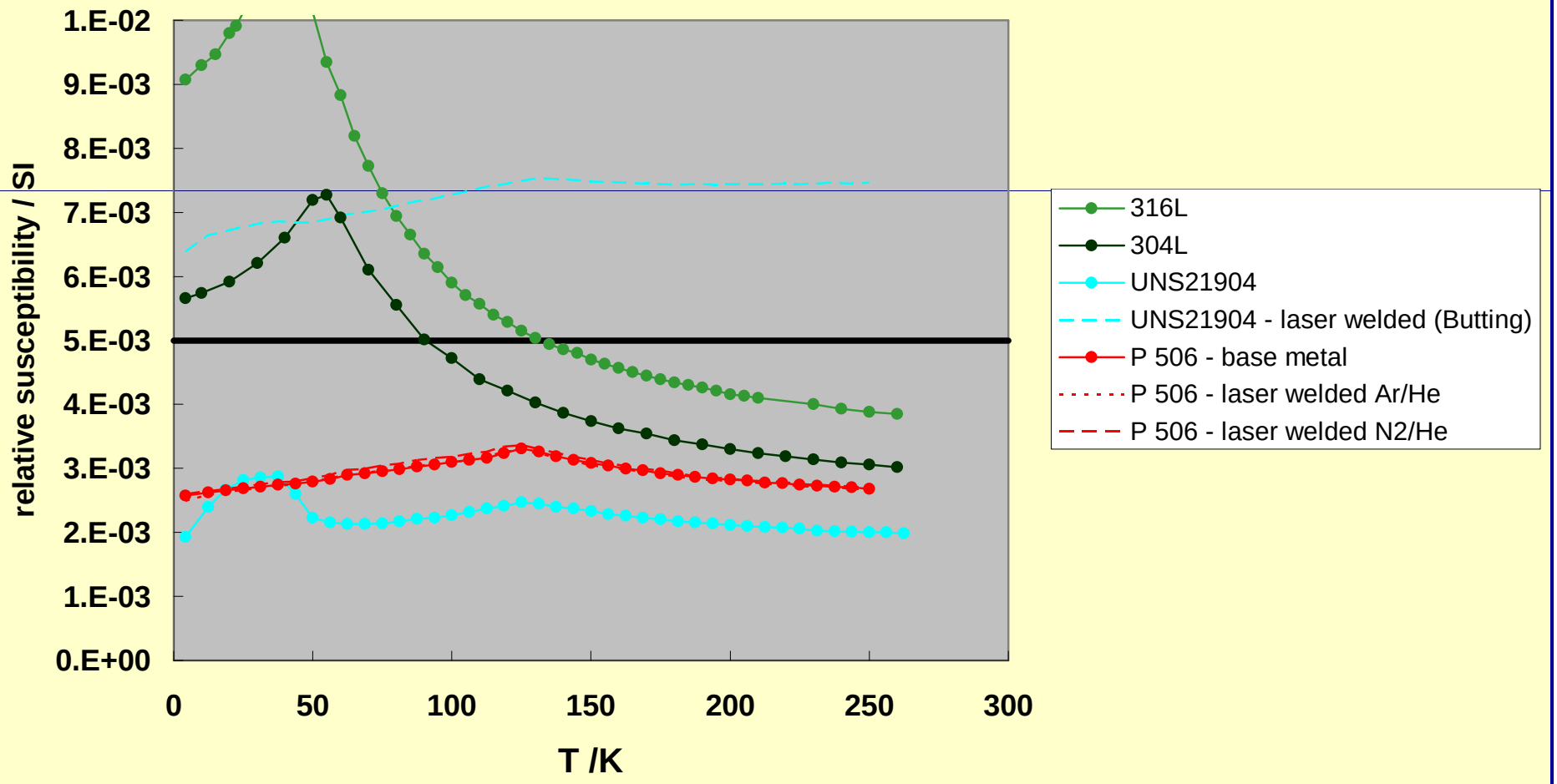

S. Sgobba and G. Hochoertler: *A New Non-Magnetic Stainless Steel for Very Low Temperature Applications,* Proc. Int. Congress Stainless Steel 1999: Science and Market, Chia Laguna /IT, 6-9 June 1999, **2**, p. 391-401

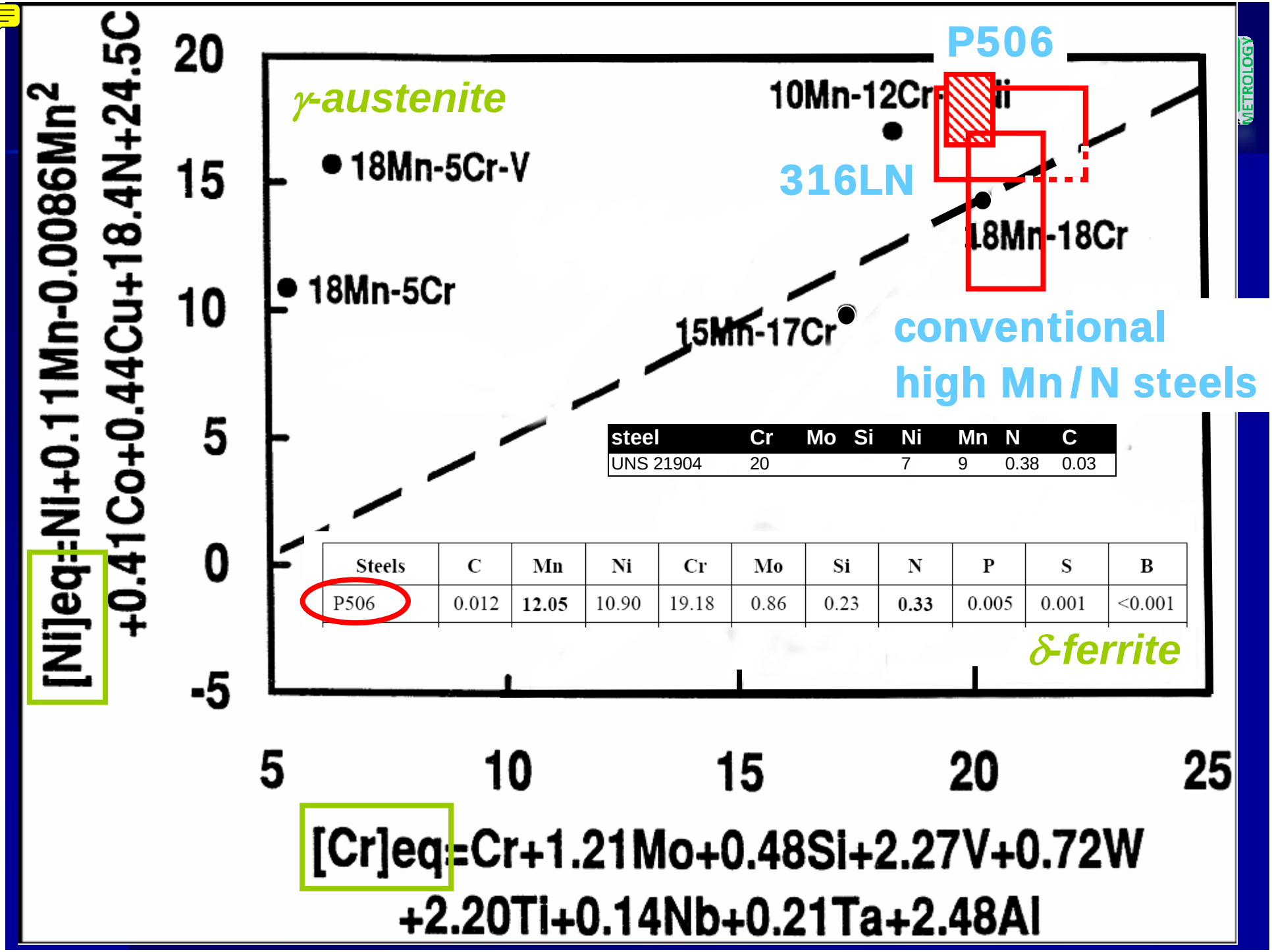

steel	Cr	Mo	Si	Ni	Mn	N	C
UNS 21904	20			7	9	0.38	0.03

Steels	C	Mn	Ni	Cr	Mo	Si	N	P	S	B
P506	0.012	**12.05**	10.90	19.18	0.86	0.23	**0.33**	0.005	0.001	<0.001

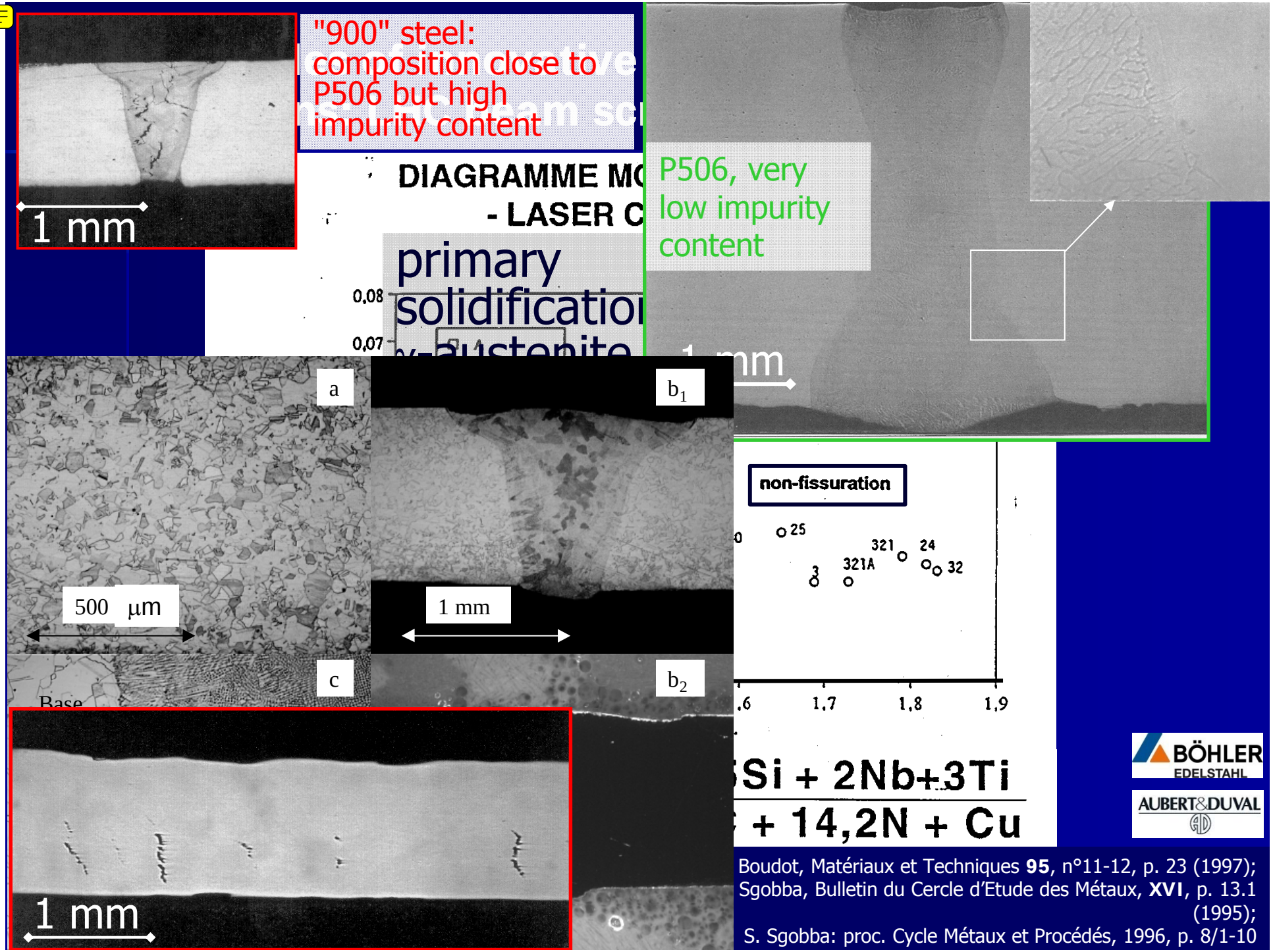

Boudot, Matériaux et Techniques **95**, n°11-12, p. 23 (1997);
Sgobba, Bulletin du Cercle d'Etude des Métaux, **XVI**, p. 13.1 (1995);
S. Sgobba: proc. Cycle Métaux et Procédés, 1996, p. 8/1-10

Thermal contraction of selected stainless steels

EDMS No. 1016843

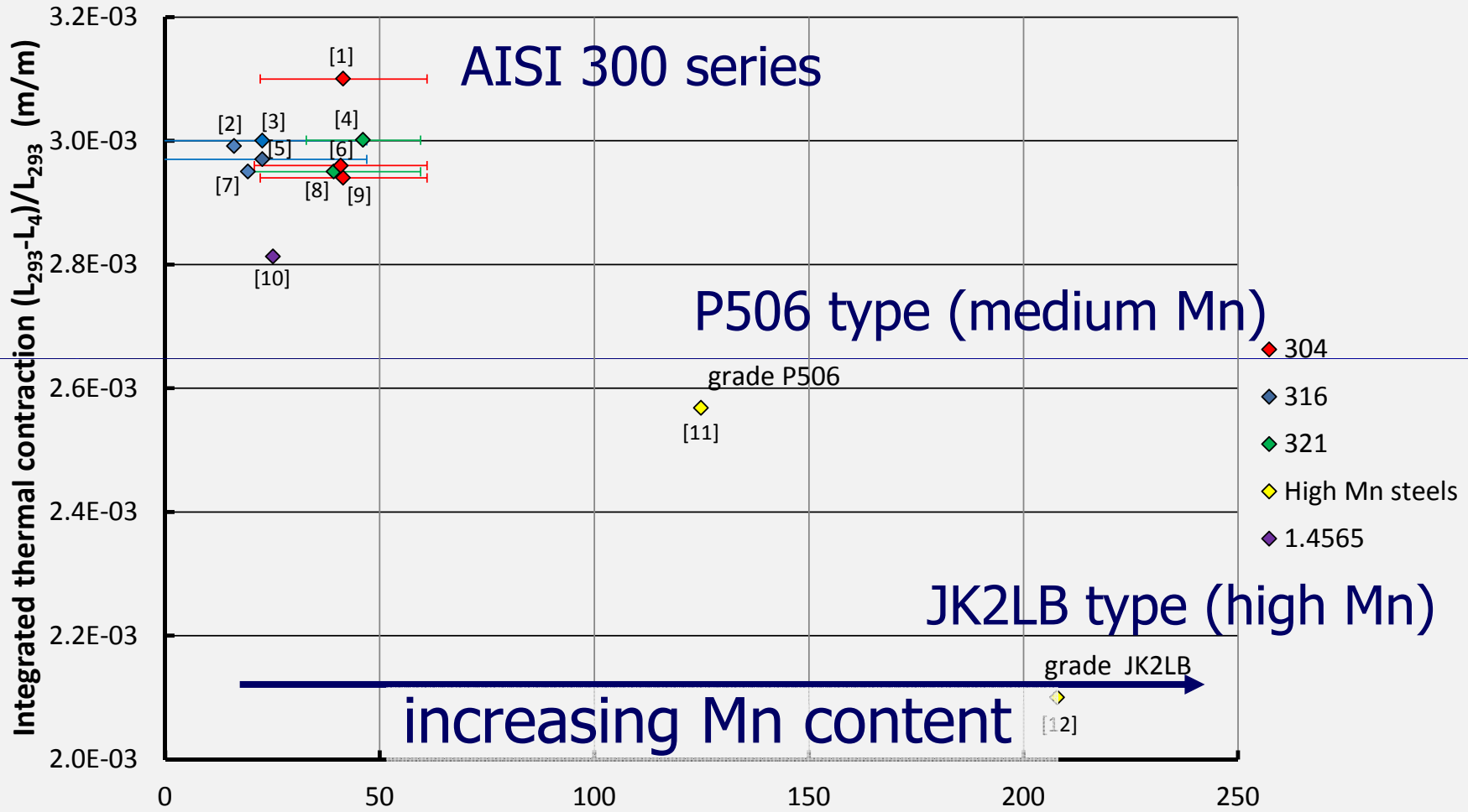

11.08.2009

Mirva Lähteenmäki
EN/MME/MM

LHC magnets, PM HIPed end covers

1997

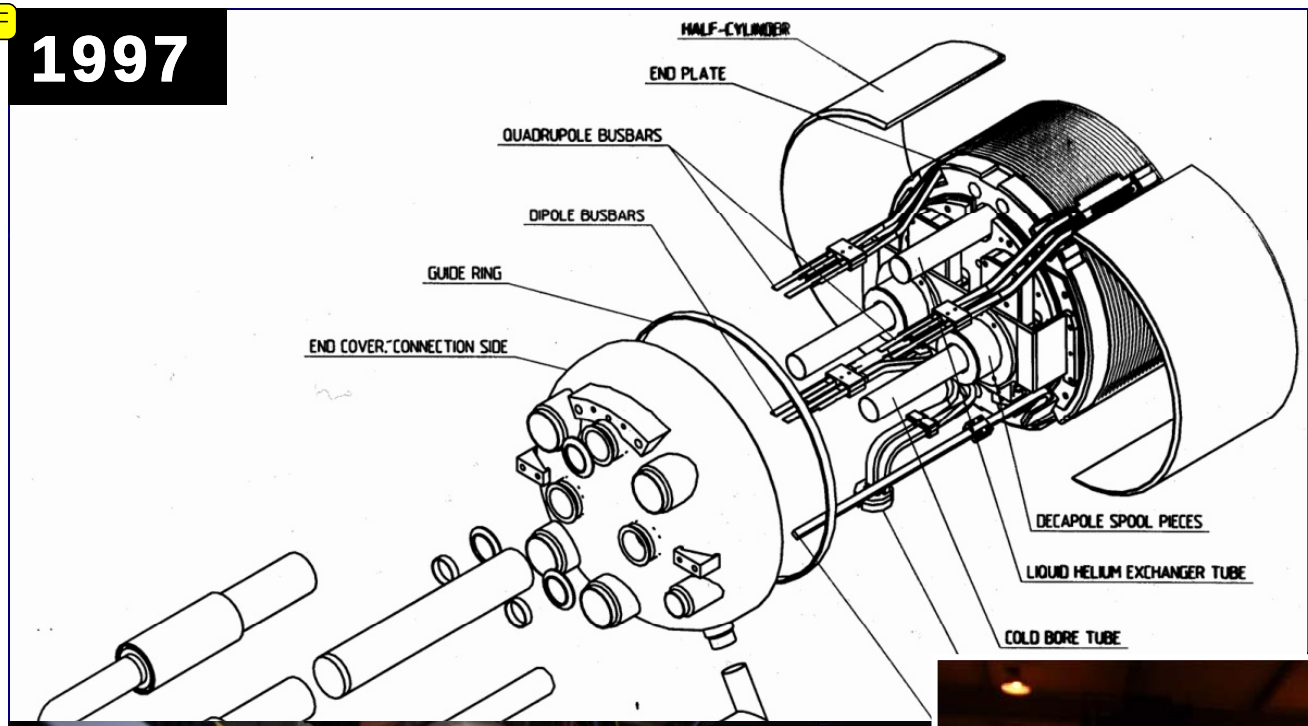

2006

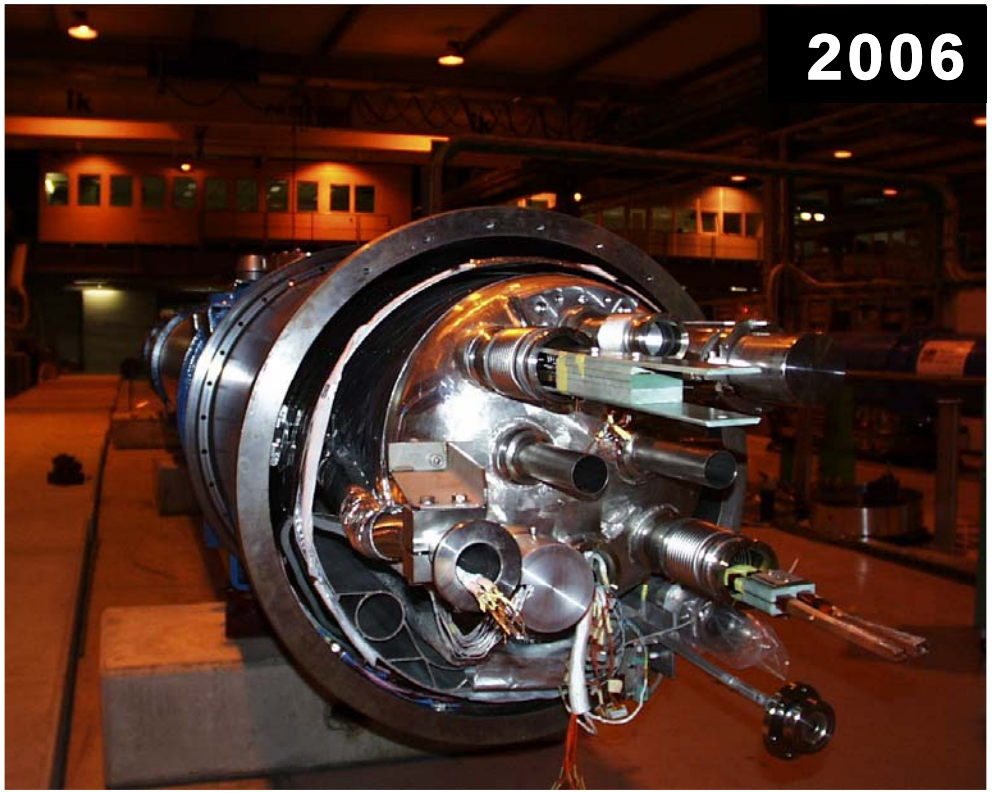

2013

LHC magnets, PM HIPed end covers

After capsule removal by pickling and solution annealing, before machining

LHC magnets, PM HIPed end covers

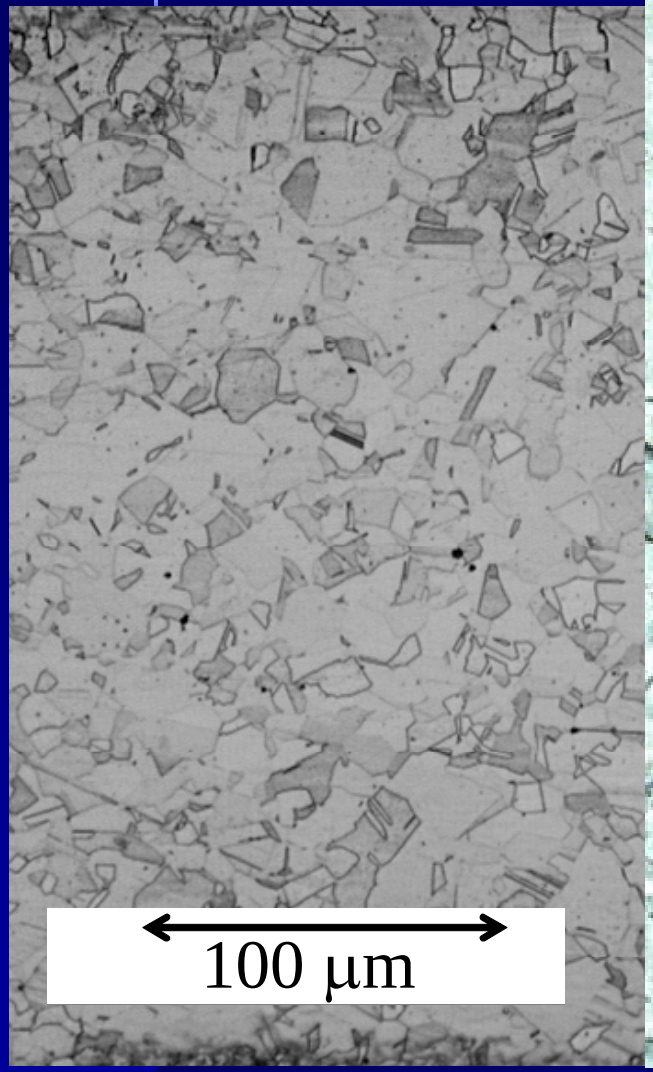

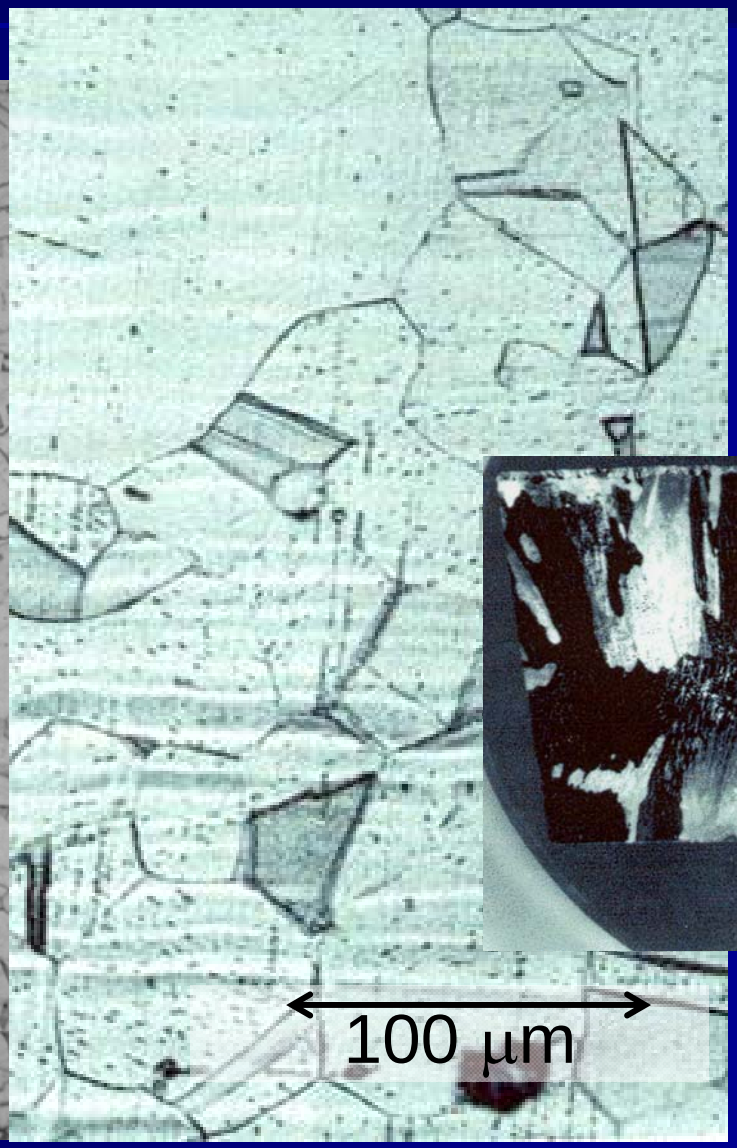

Price competitive compared to wrought and cast

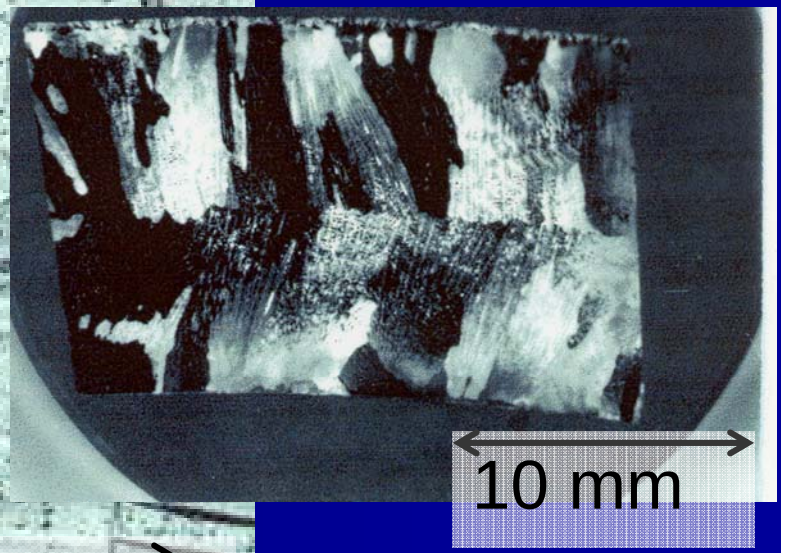

LHC magnets, PM HIPed end covers

HIPed PM 316LN		Metso	CERN Specification	
		H 6277	*Min.*	*Max.*
Composition (w%)	C	**0.017**		0.030
	Si	**0.59**		1.00
	Mn	**0.71**		2.00
	S	**0.005**		0.015
	P	**0.012**		0.040
	Ni	**13.07**	12.00	14.00
	Cr	**16.98**	16.00	18.00
	Mo	**2.53**	2.00	3.00
	O	**0.011**		
	N	**0.185**	0.15	0.20

Typical Oxygen levels

in 316LN:	Couturier et al. (1998)	**200 ppm**
	Dellis et al. (1996)	**195 ppm**
in 304L:	Appa Rao and Kumar. (1997)	**400 ppm**
in aust. SS	Zou and Grinder (1982)	**300 to 4500 ppm**
in 304L	Dunkley (1981)	**1200 to 7800 ppm**

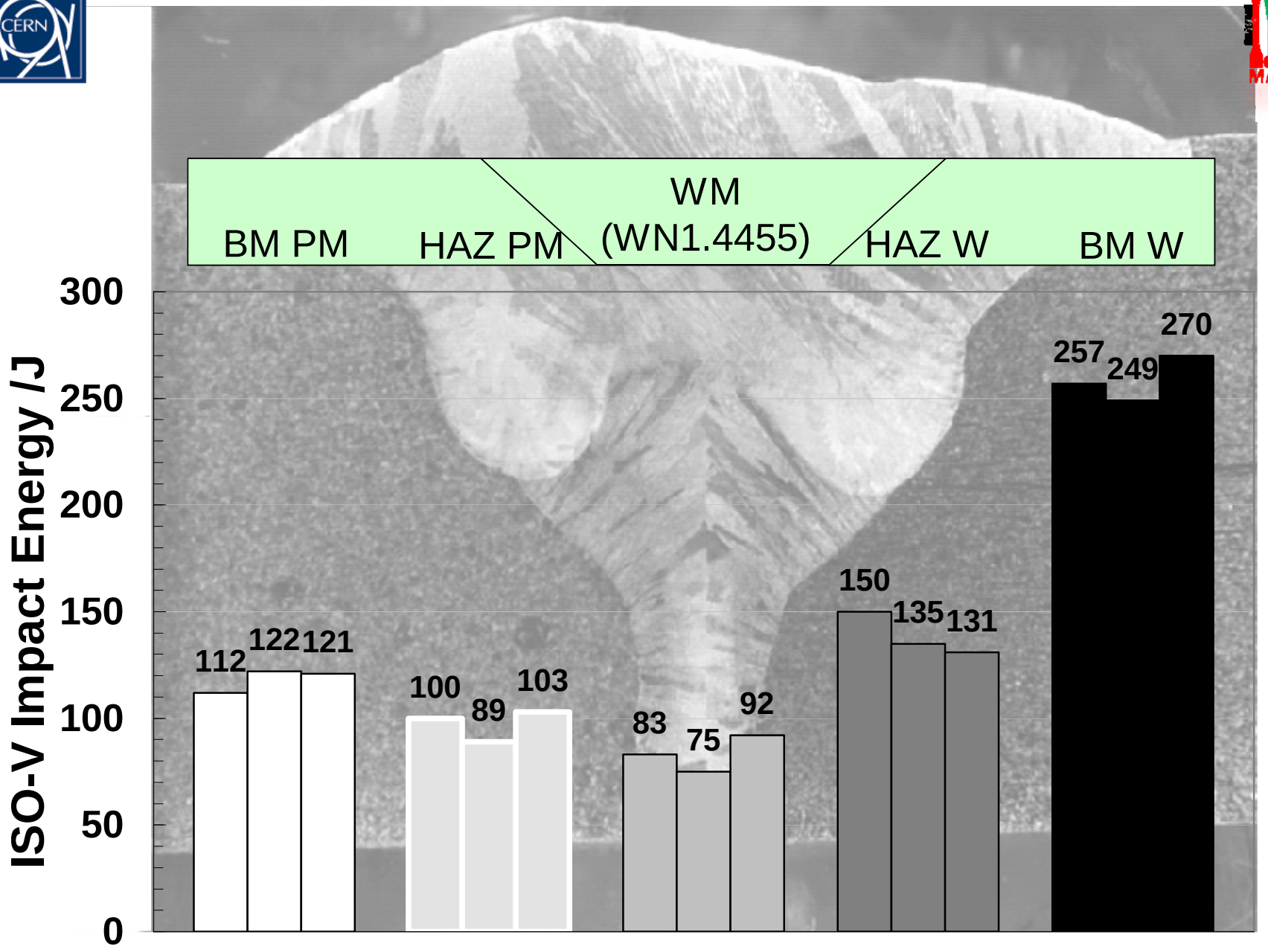
BM PM
HAZ PM
WM
(WN1.4455)
HAZ W
BM W
ISO-V Impact Energy /J
300
250
200
150
100
50
0
112
122
121
100
89
103
83
75
92
150
135
131
257
249
270

LHC magnets, PM HIPed end covers

Fractographic analysis

Oxides within dimples

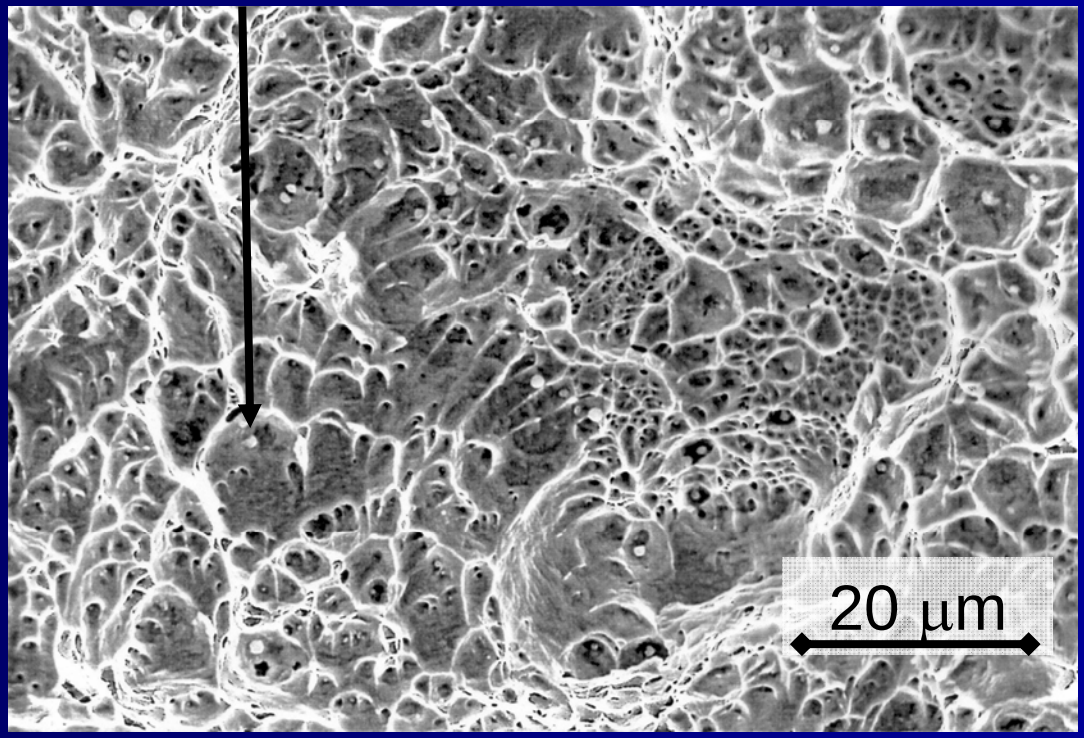

Localized ductility (Couturier 99)

METAL POWDER INDUSTRIES FEDERATION

MPIF

PM Design Competition Award Winner

Award: Grand Prize
Year: 2007

Description:
The award was given to an end cover is used in the Large Hadron Collider, the world's largest and highest energy sub-atomic particle accelerator. Made from 316LN stainless steel powder, the part is hot isostatically pressed to full density. The superconducting dipole cryomagnets operate in a cryogenic environment at minus 450°F. As HIPed to a near-net shape of 253.5 pounds, the finished end cover weighs 153.3 pounds. The fabricator incorporated finite element analysis, computer aided design, numerically controlled sheet metal cutting technology, and cutting-edge robotic welding and part manipulation to produce the end covers. This resulted in a more-than-50-times increase over the typical production rate of fully-dense HIPed PM near-net shapes, an unprecedented breakthrough in productivity. About 2,700 end covers have been delivered to CERN. The design of the part features several complex configurations. For example, both the inner and outer surface of the broad face is radiused with the inner surface approximately parallel to the outer surface. The exterior of the curved surface has either eight or 10 projections, depending upon which version of the part is produced. The design differs slightly depending on which side of the dipole magnet it is located. The PM HIPed part meets the equivalent mechanical properties of 316LN wrought stainless steel, including internal toughness and high ductility.

Part: Dipole Cryomagnet End Cover
Fabricator: Bodycote HIP-Surahammar
End User: Metso Materials Technology Oy for CERN

LHC experiments, the CMS example:
reinforcement of the Al-stabilized conductor

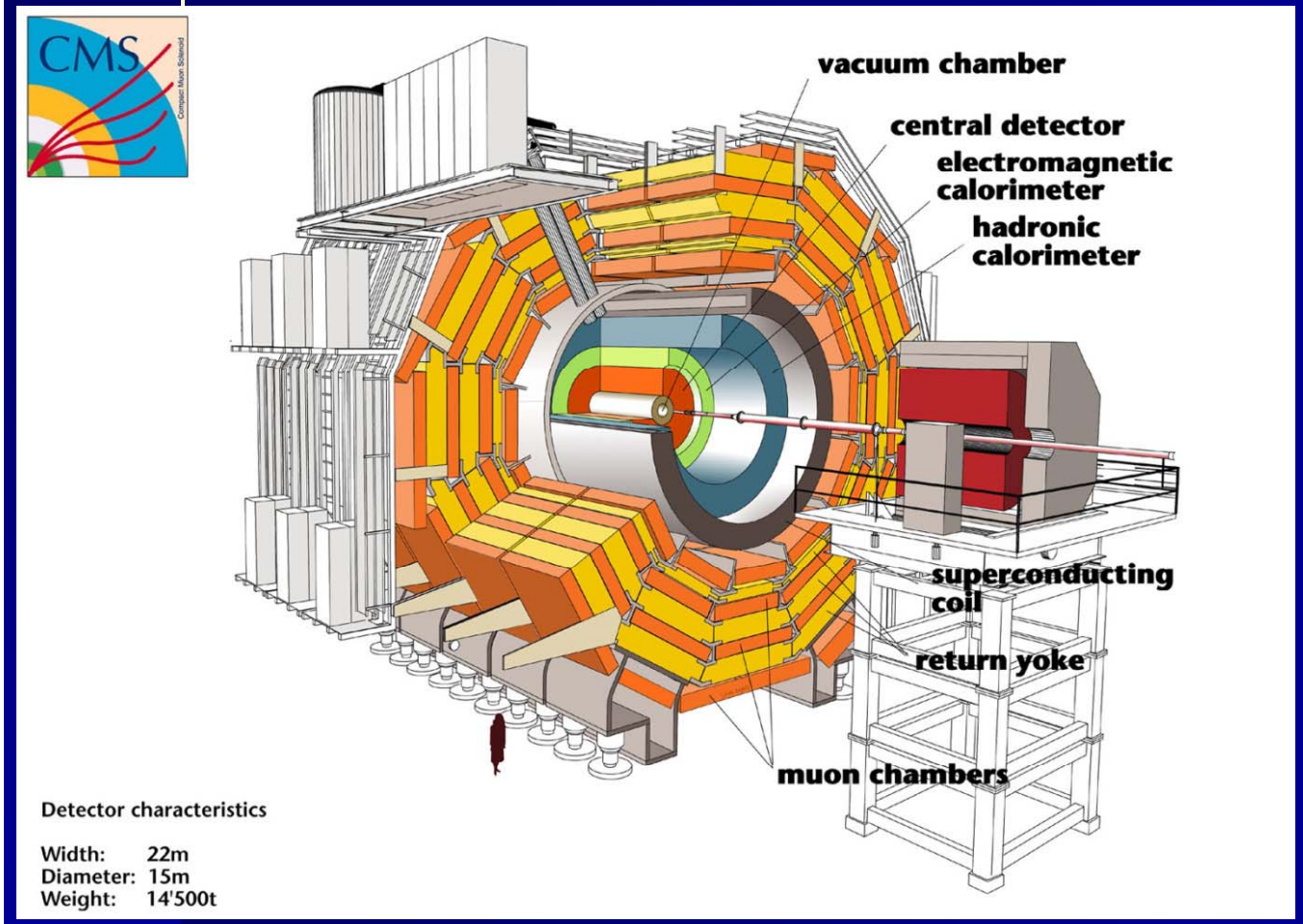

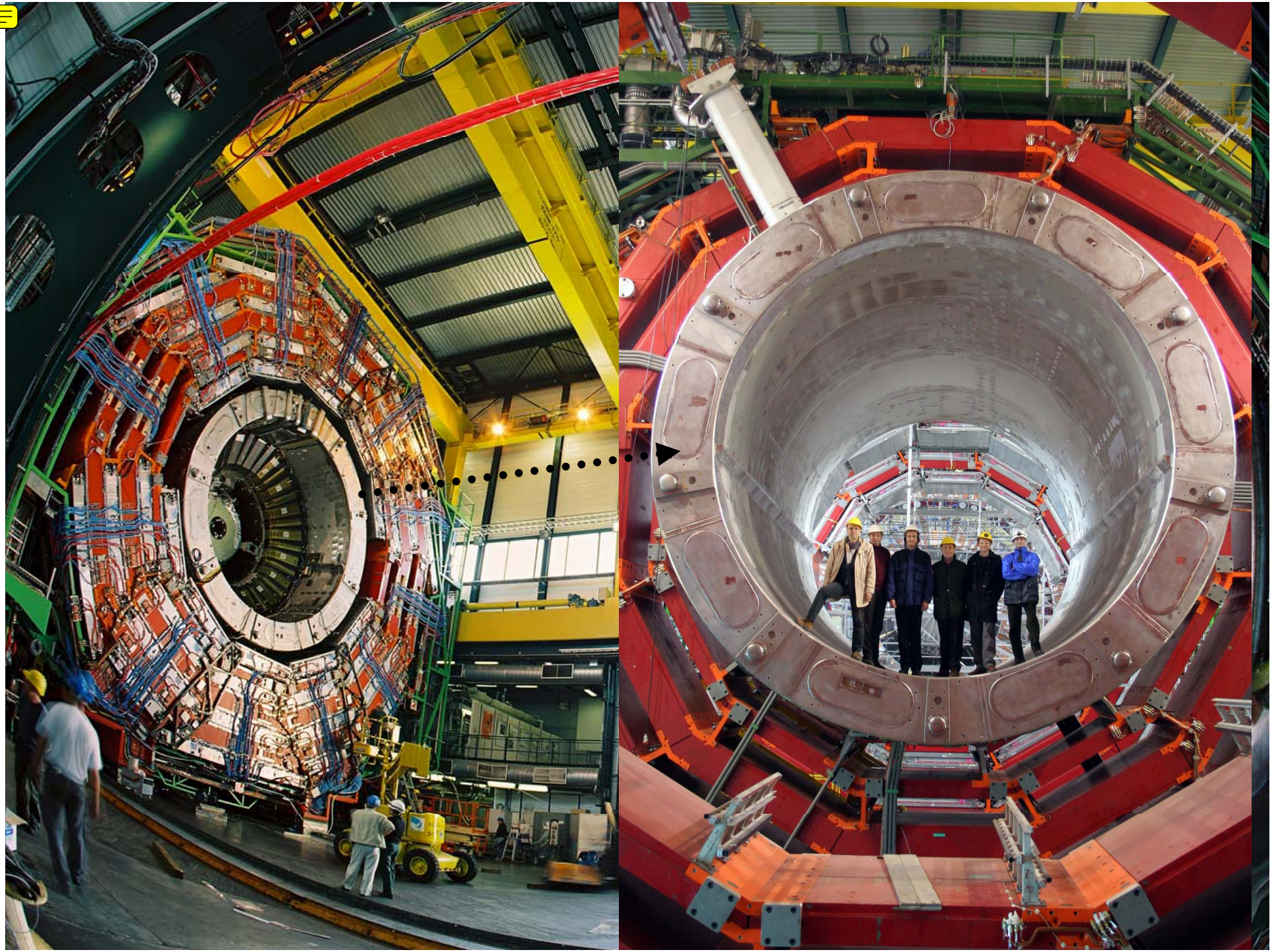

E/M ratio vs. E for several solenoids

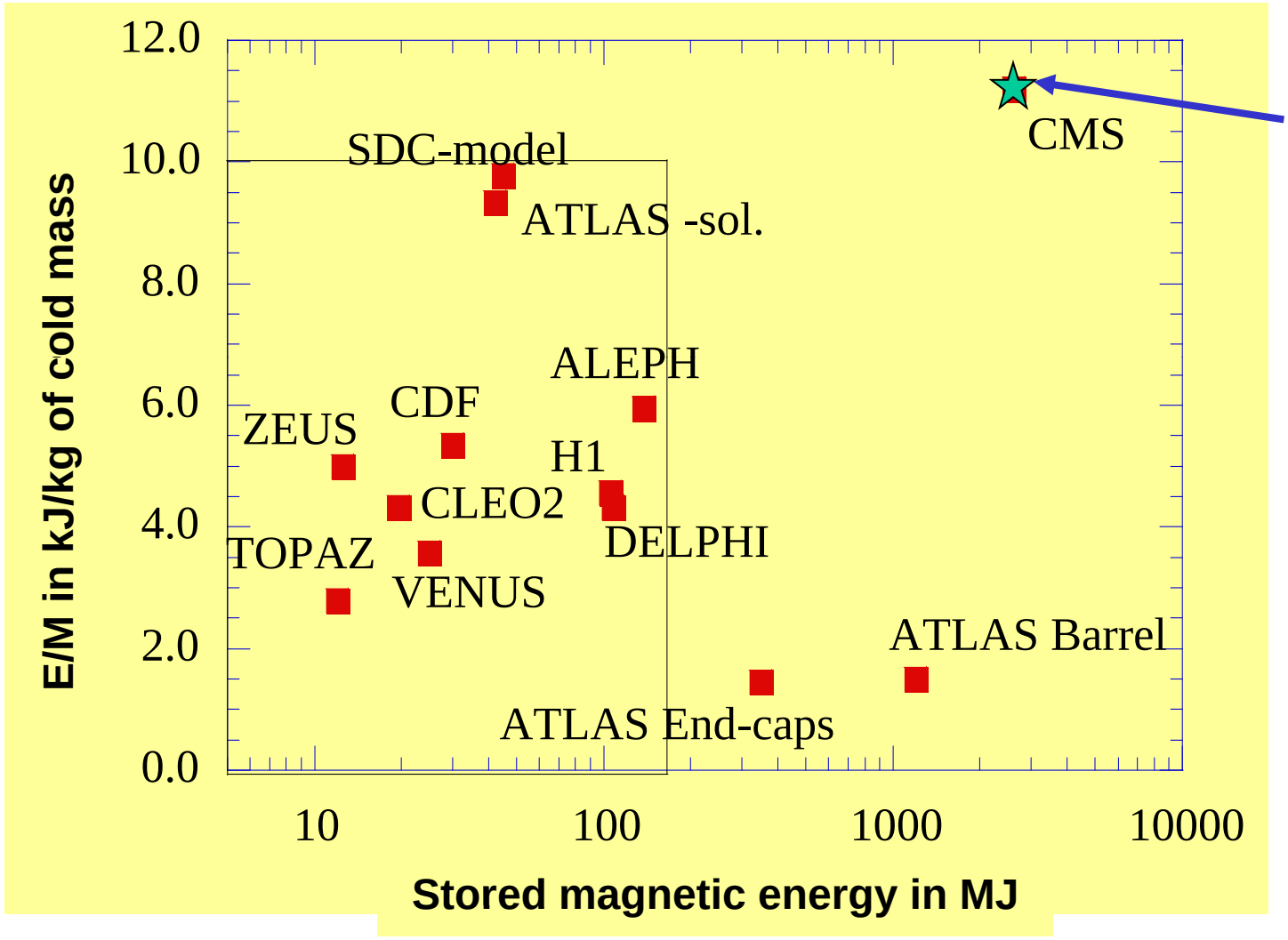

This 'anomalous' positioning meant that innovative solutions were needed to face this challenge

Alain Hervé et al., MT20 in Philadelphia, 27 August 2007

LHC experiments, the CMS example:
reinforcement of the Al-stabilized conductor

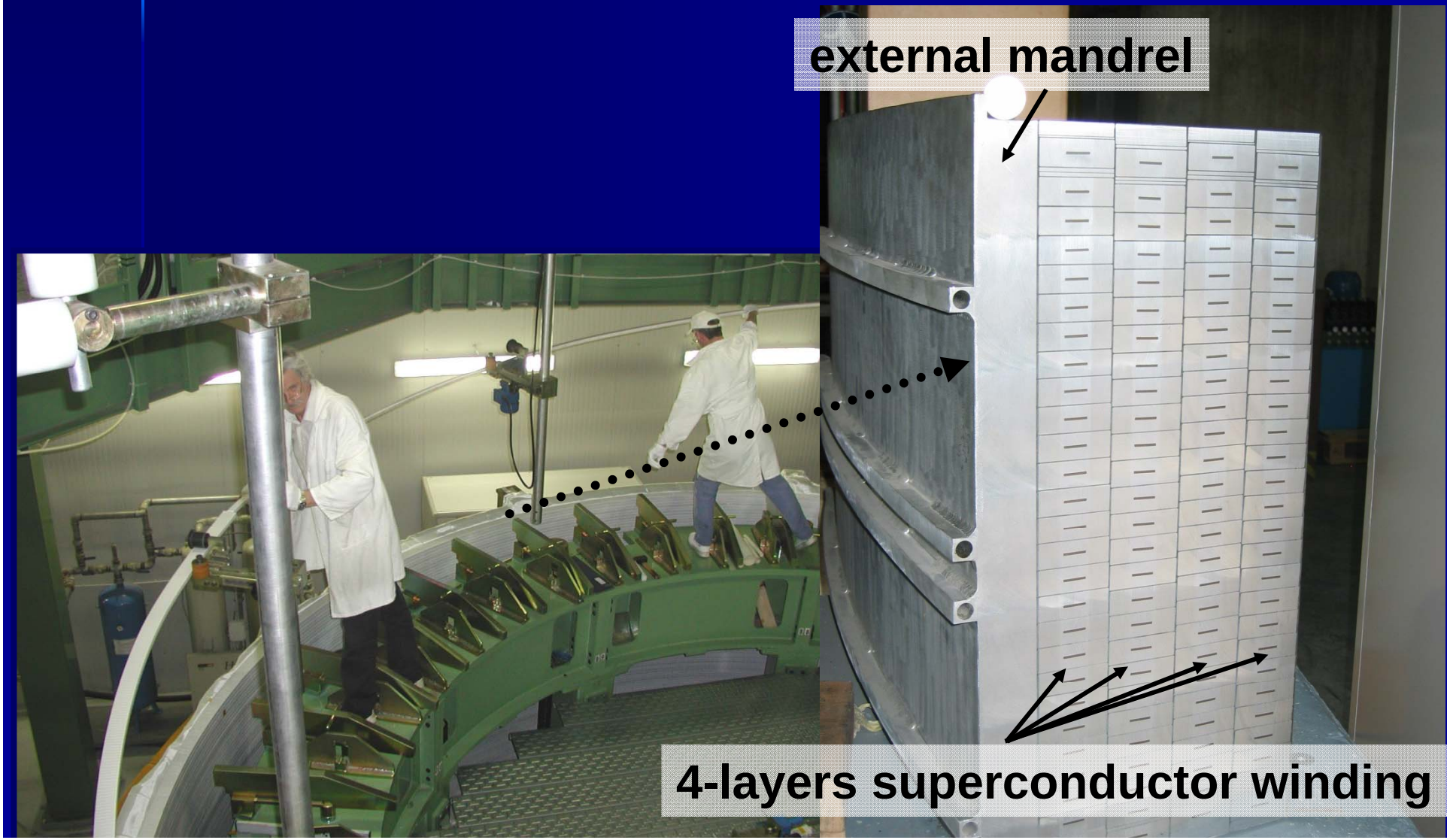

LHC experiments, the CMS example: reinforcement of the Al-stabilized conductor

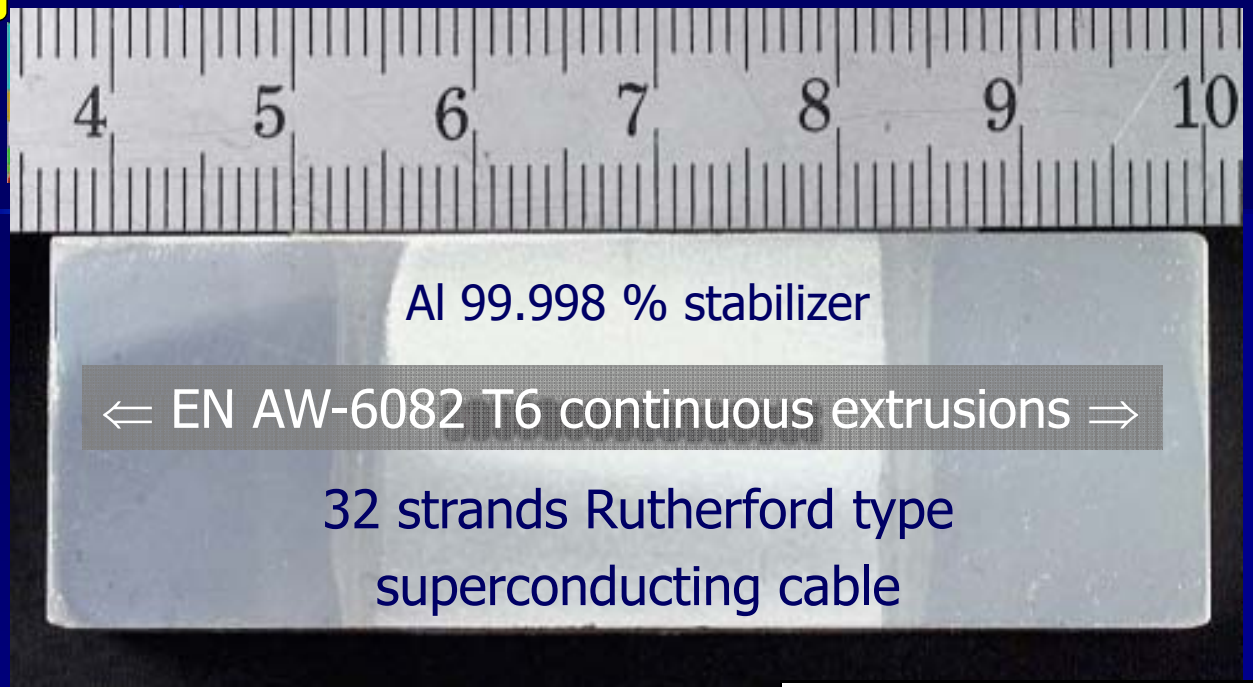

Reinforcement Insert

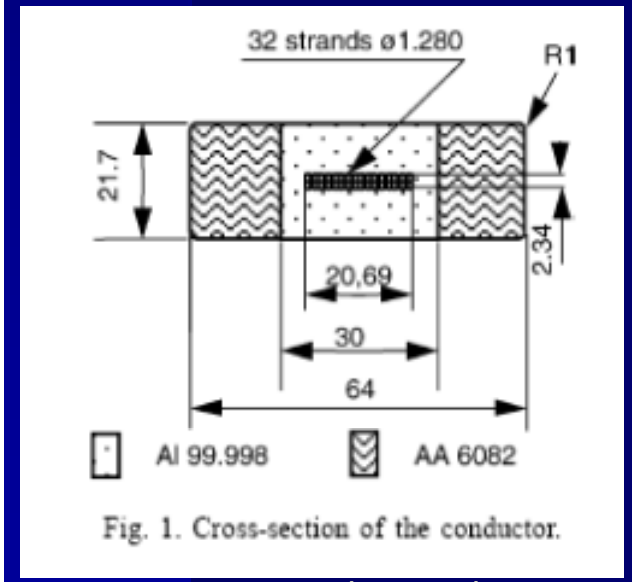

Fig. 1. Cross-section of the conductor.

Nominal current	**20 kA**
Superconducting strand type	**NbTi- Cu stabilized**
Strand Cu/SC ratio	**1.1**
Number of strands	**32**
Strand diameter	**1.28 mm**
Rutherford cable cross section	**20.68 mm x 2.34 mm**
Insert cross section	**30 mm x 21.6 mm**
High Purity Aluminum stabilizer	**Al 99.998 %**
RRR aluminum at 0 T, annealed	**> 1500**
Reinforcement material	**EN AW-6082**
Conductor cross section	**64 mm x 21.6 mm**
Quantity produced	**21 lengths x 2600 m**

structural materials

LHC experiments, the CMS example
billet on billet extrusion of the reinforcement

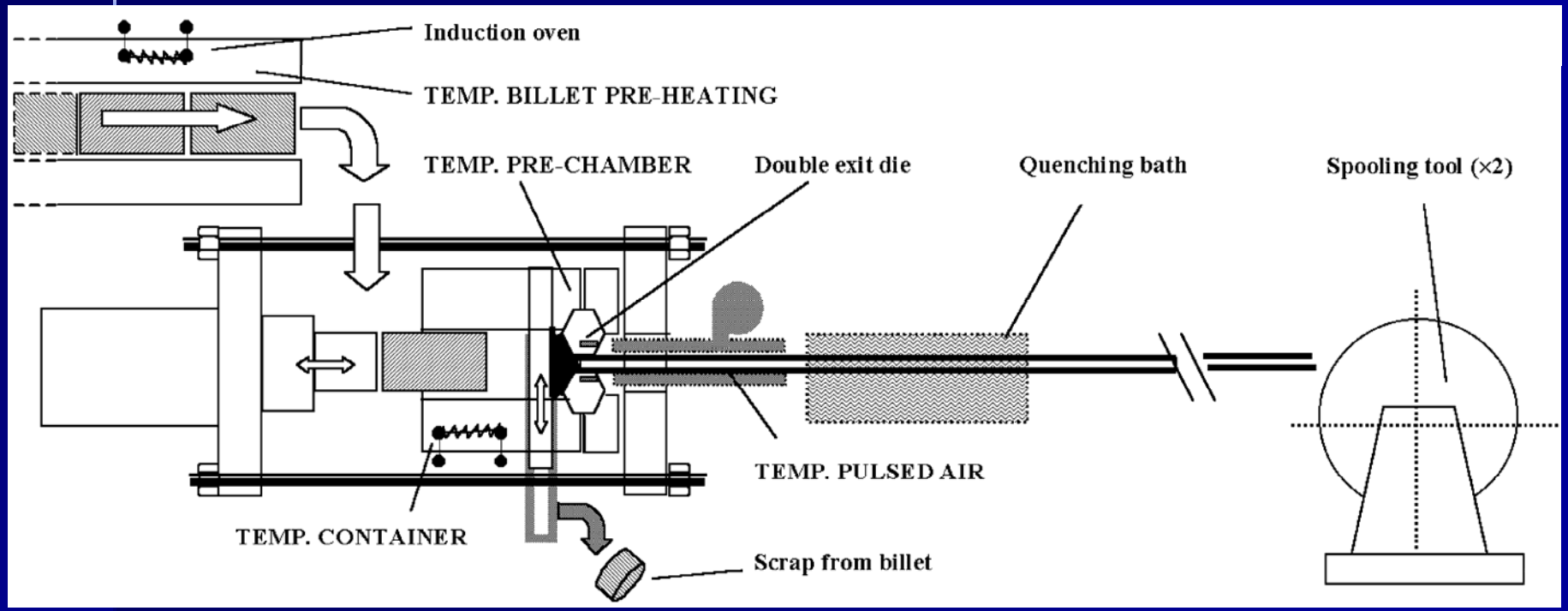

Schematic representation of the extrusion line (S. Sequeira Tavares, S. Sgobba, *An improved billet on billet extrusion process of continuous aluminium alloy shapes for cryogenic applications in the Compact Muon Solenoid experiment*, J. of Mat. Proc. Technology 143–144 (2003) 584–590)

LHC experiments, the CMS example
billet on billet extrusion of the reinforcement

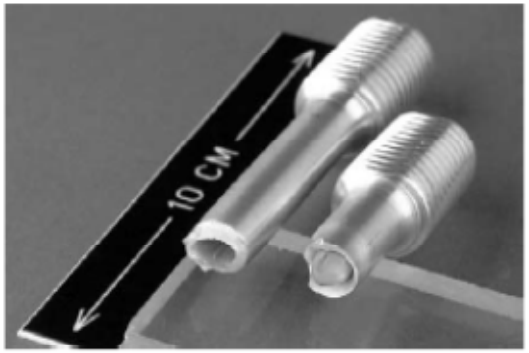

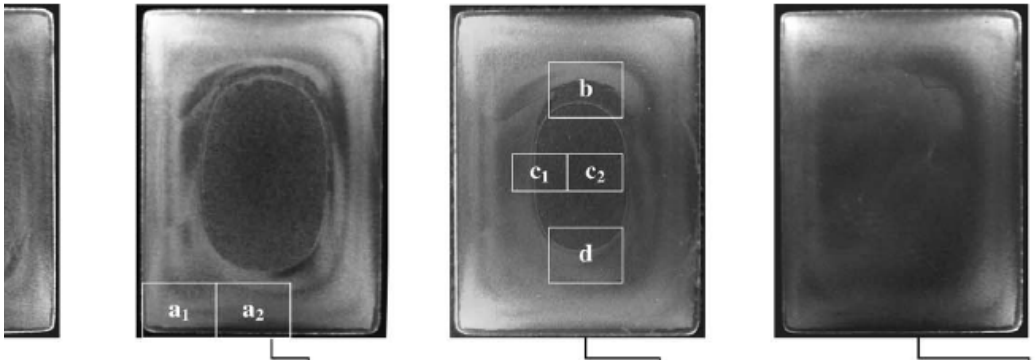

Fig. 8. Fracture of a tensile specimen containing a transverse weld.

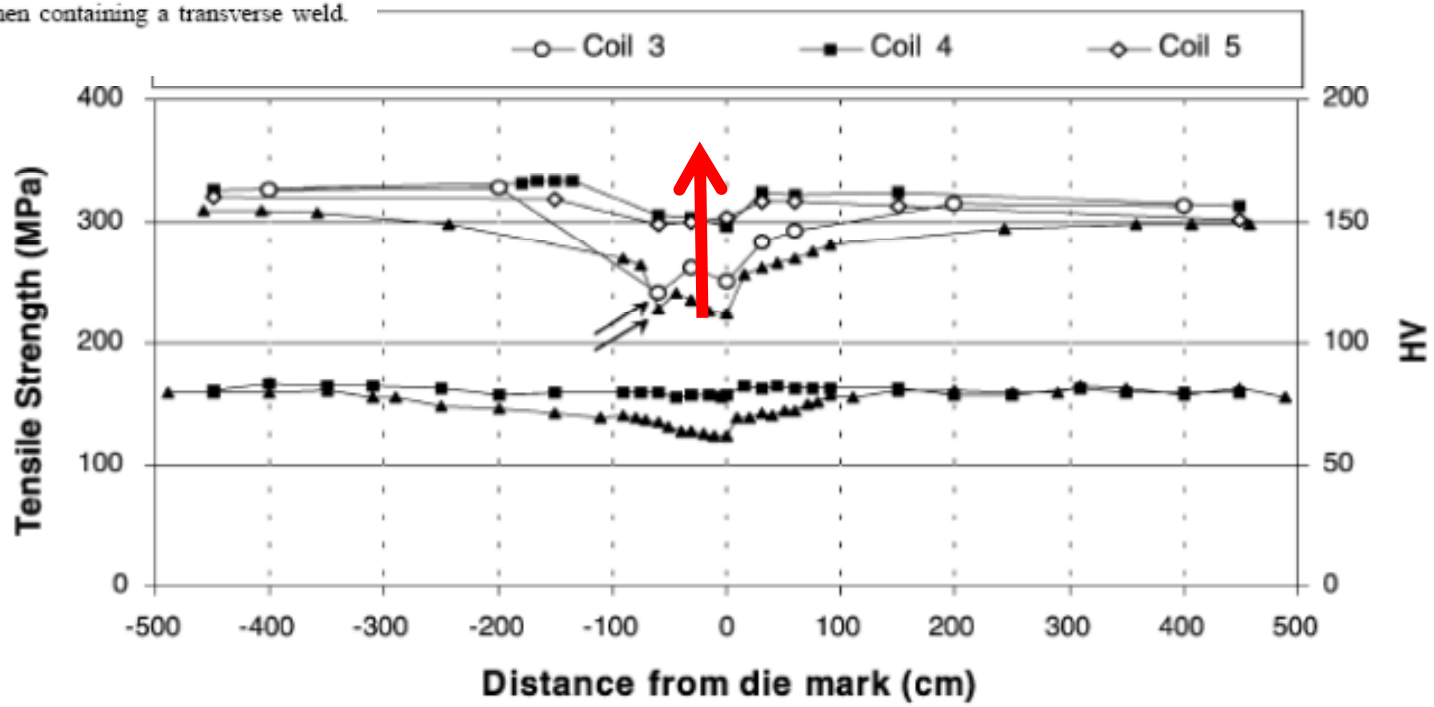

LHC experiments, the CMS example
billet on billet extrusion of the reinforcement

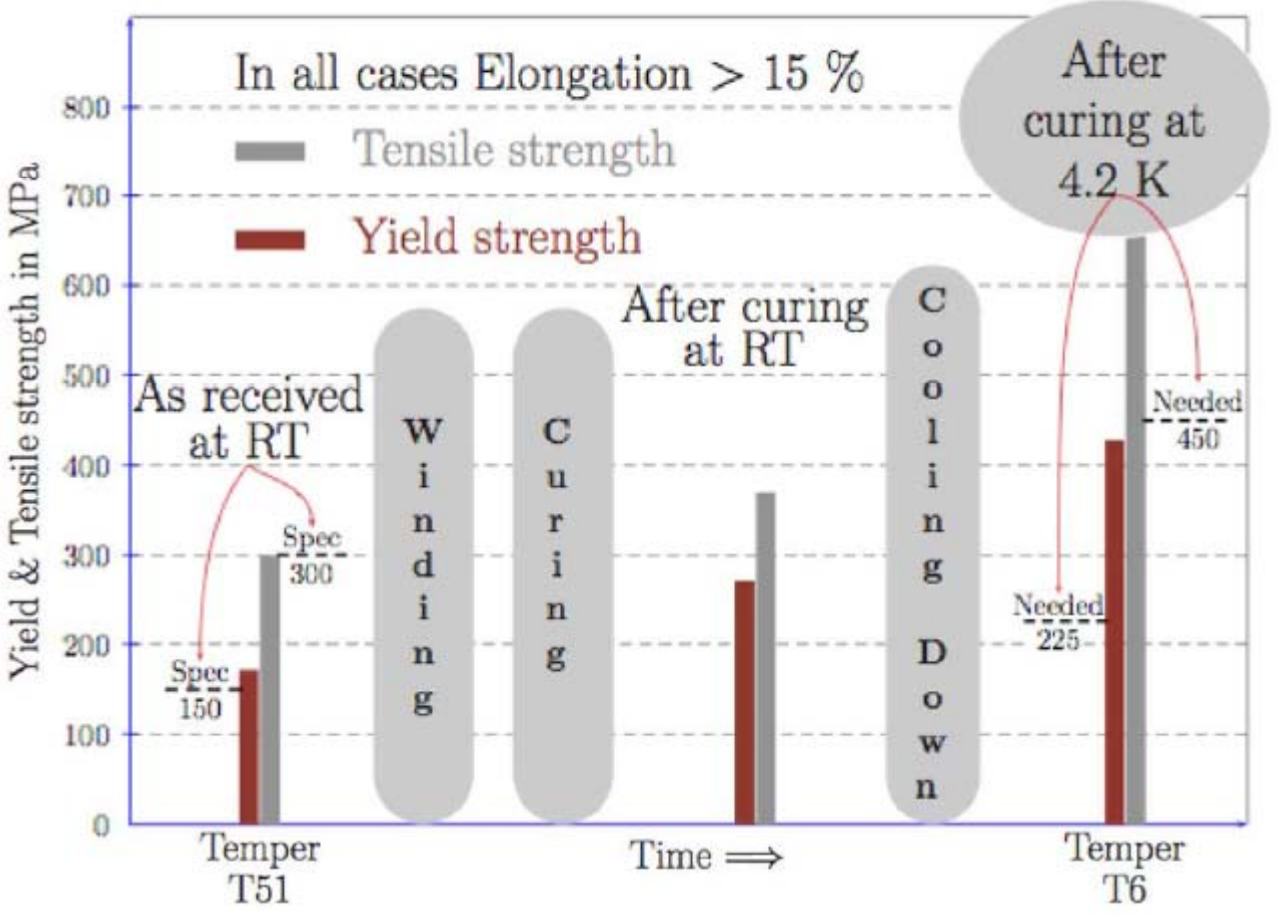

Alain Hervé et al., MT20 in Philadelphia, 27 August 2007

Evolution of the mechanical properties of the alloy 6082 selected for the reinforcement of the conductor, from state T51 to T6 at RT and 4.2 K.

Candidate alloy:

- Al99.998 ⇒ Al-0.1wt%Ni
- developed for the ATLAS thin solenoid superconductor
- maintains $Rp_{0.2}$ = 85 MPa at 4.2 K after thermal cycle

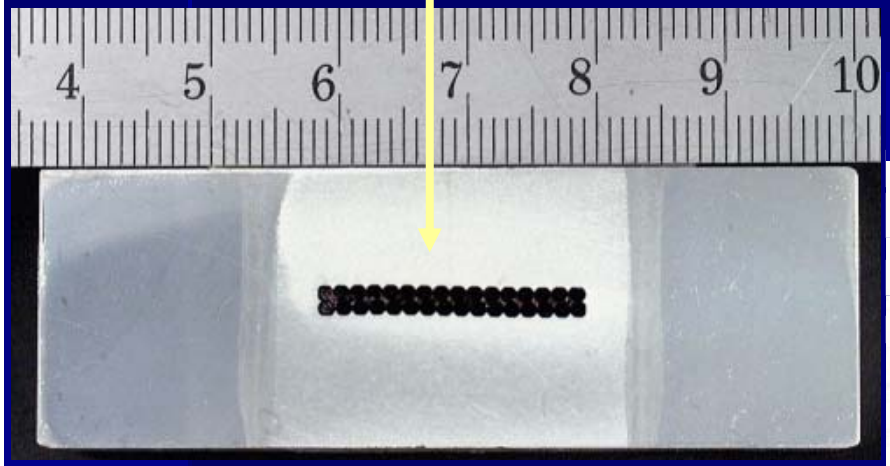

A. Yamamoto et al., Nuclear Physics B 78 (1999), pp. 565-570;
Wada et al., *IEEE Trans. Appl. Superconduc.*, vol. 10, pp. 373-376, March 2000

Selection and properties of structural materials

T or 6 T,
s:

50 MPa ⇒

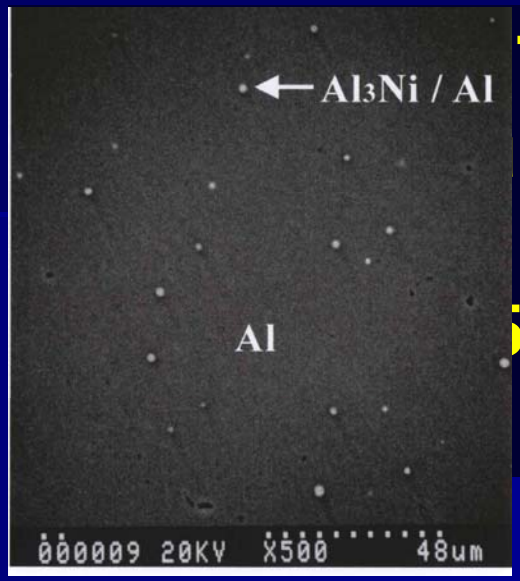

S. Sgobba et al., *IEEE Trans. Appl. Superconduc.*, vol. 16, p. 521, June 2006

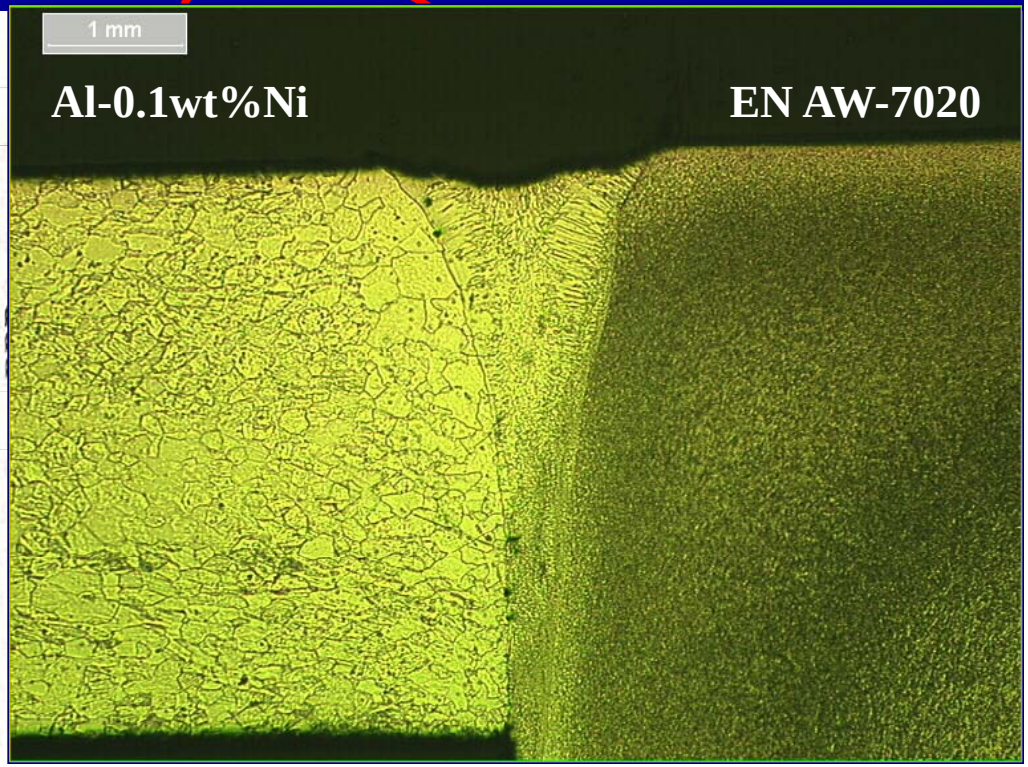

Ongoing developments:
innovative materials for conductors of future particle experiments

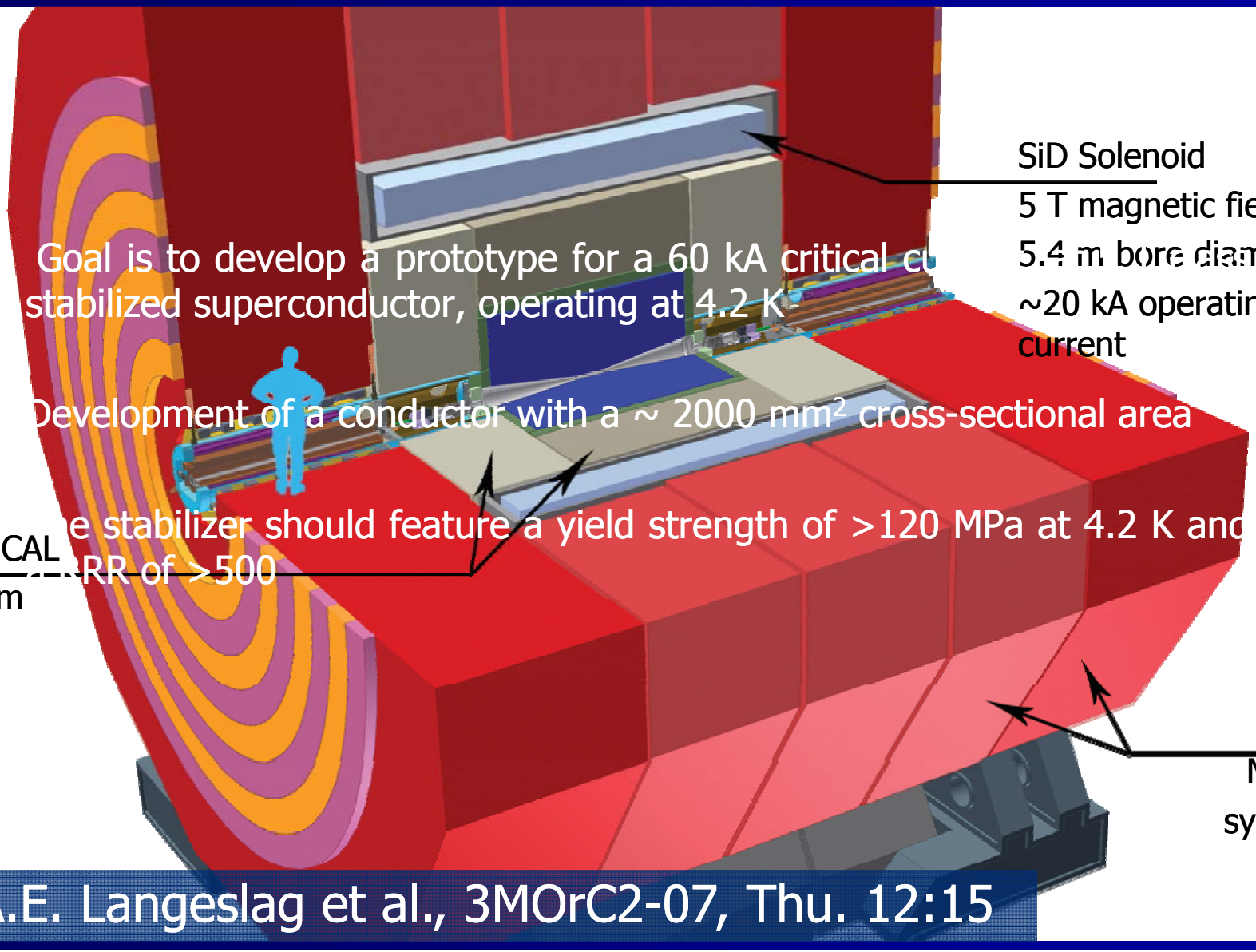

Goal is to develop a prototype for a 60 kA critical cu
stabilized superconductor, operating at 4.2 K

Development of a conductor with a ~ 2000 mm² cross-sectional area

e stabilizer should feature a yield strength of >120 MPa at 4.2 K and
RR of >500

⇒ S.A.E. Langeslag et al., 3MOrC2-07, Thu. 12:15

gress of Al-stabilized SC

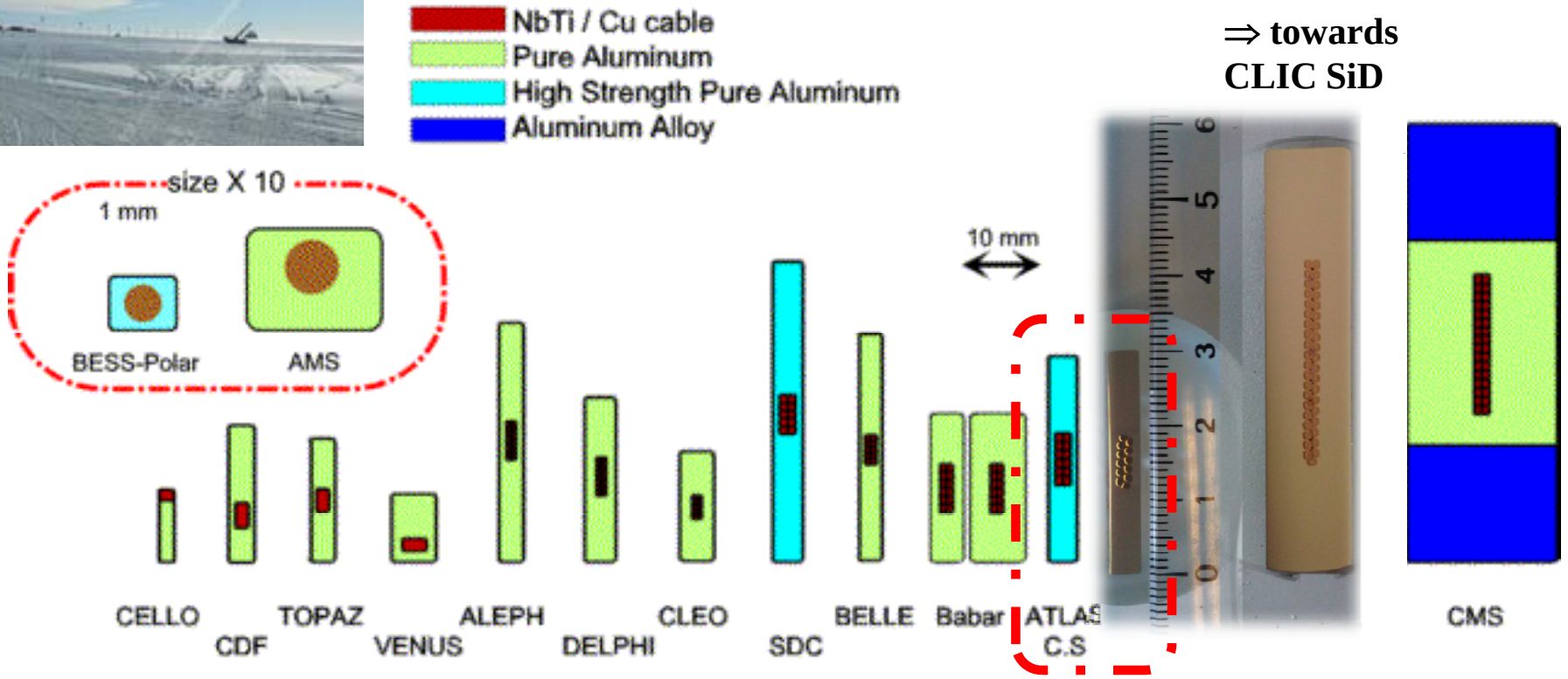

A. Yamamoto, "Advances in Superconducting Magnets for Particle Physics", *IEEE Trans. Appl. Superconduc.*, vol. 14, no. 2, pp. 477-484, June 2004.

⇒ S.A.E. Langeslag et al., 3MOrC2-07, Thu. 12:15

LHC experiments, the CMS example: external cylinder

Flanges, including shoulders

Welded shell

Selection and properties of structural materials

Ongoing developments: selection and characterization of structural materials for fusion magnets

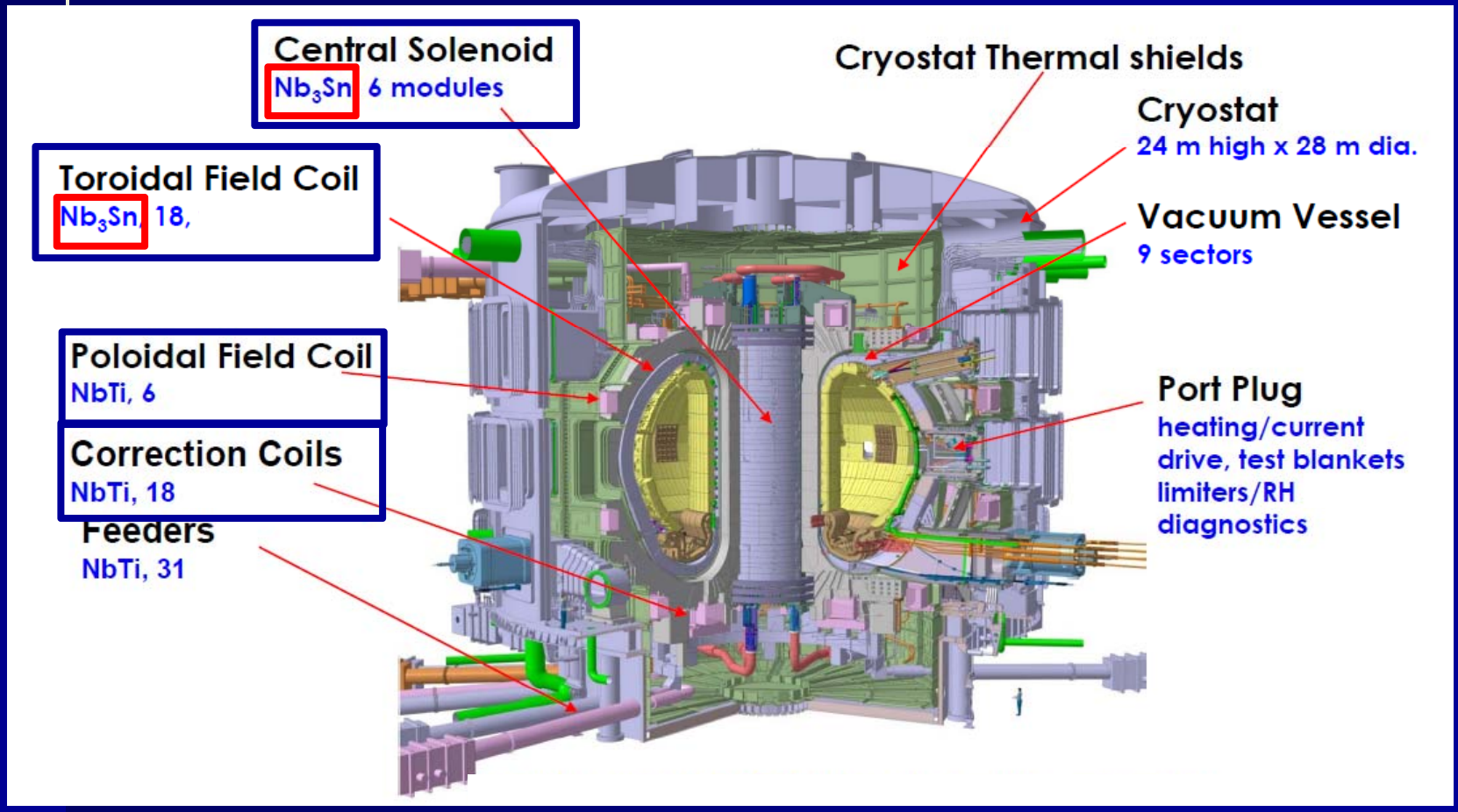

N. Mitchell, A. Devred, P. Libeyre, B. Lim, F. Savary and the ITER Magnet Division The ITER Magnets: Design and Construction Status, presentation at MT-22, Marseille,13 Sept 2011. See also: N. Mitchell et al., The ITER Magnet System, IEEE Trans. Appl. Superconductivity **18** (2008) 435.

Selection and characterization of structural materials for fusion magnets

The ITER central Solenoid, CS coil cutaway view

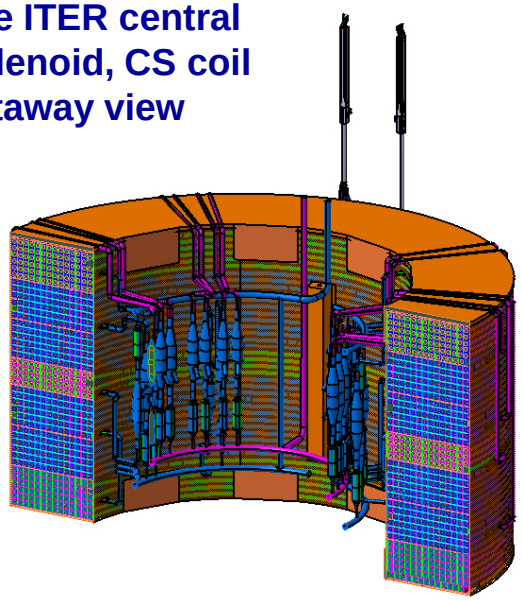

ITER CS includes six identical coils called modules

Use a superconducting 40 kA Nb_3Sn cable-in-conduit conductor operating up to 13 T, stacked upon each other and surrounded by a vertical precompression structure

Pulsed operation: 60 000 cycles !

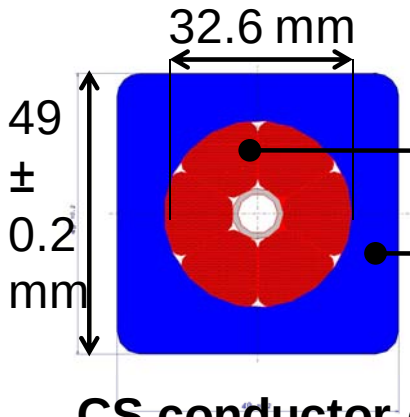

CS conductor cross-section

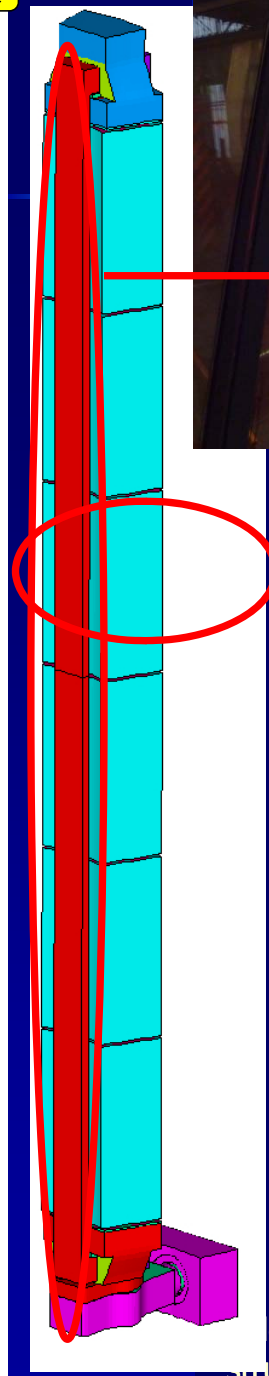

courtesy of Kind /DE

.484E+09
.518E+09
.551E+09
.584E+09
.618E+09

/Pa

Stainless steel grades considered for prototype production:

316LN, ITER grade

JK2LB, high Mn grade

P. Libeyre, D. Bessette, A. Devred, C. Jong, N. Mitchell, S. Sgobba, *Manufacturing development to meet the mechanical requirements of the ITER Central Solenoid Coils*, Proceedings of the 26th Symposium on Fusion Technology (SOFT), Porto (PT), 2010, also: *Fusion Eng. Des.* **86** (2011), 1553–1557.

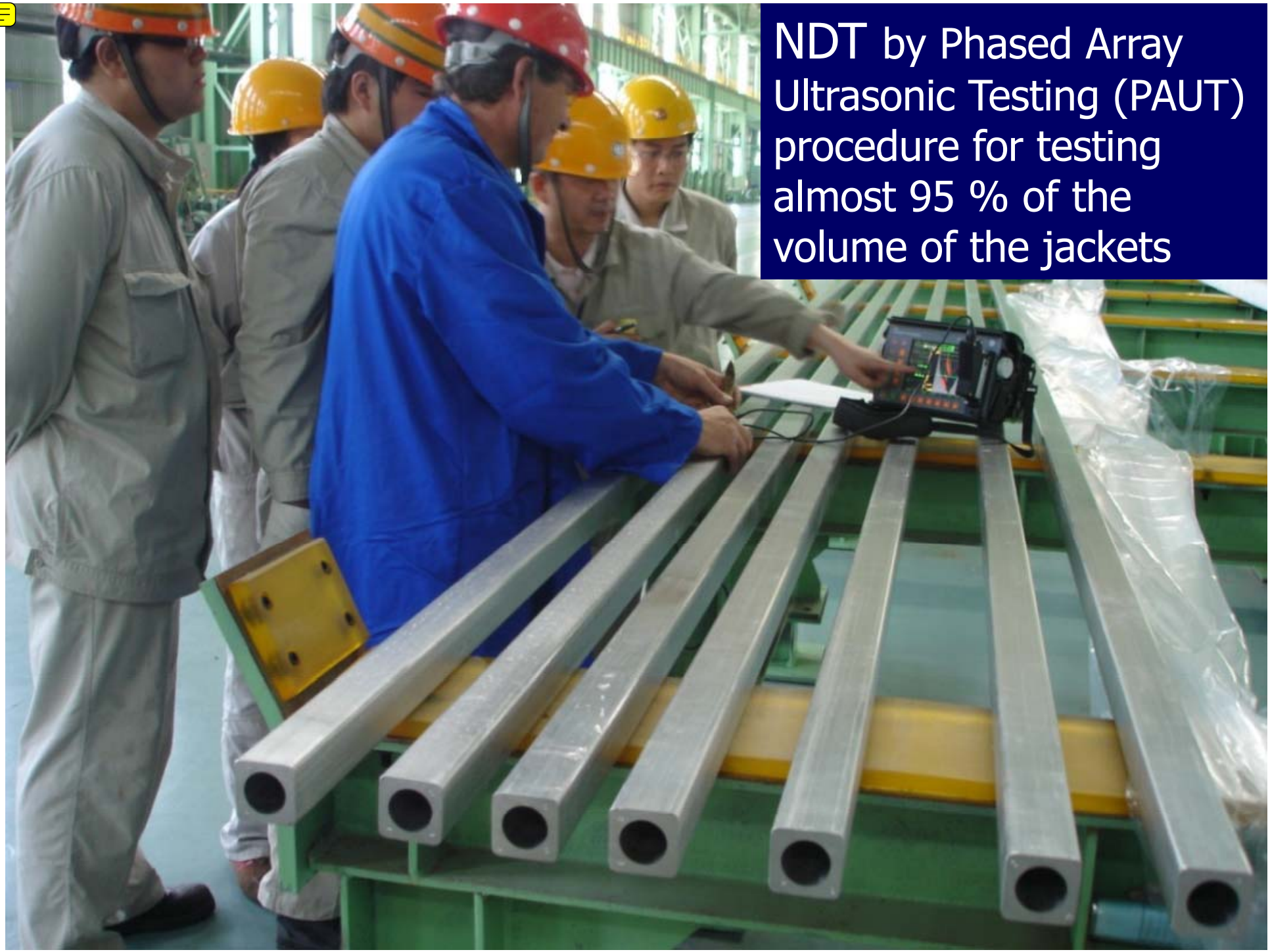
NDT by Phased Array Ultrasonic Testing (PAUT) procedure for testing almost 95 % of the volume of the jackets

Table 1a. Chemical composition of JK2LB

Element (wt%)	C	Si	Mn	P	S	Cr	Ni	Mo	N	Co	B
JK2LB	≤0.030 (Target <0.025)	≤0.50 (target< 0.28)	20.5 - 22.5	≤0.015 (target <0.008)	≤0.015 (target <0.008)	12.0 - 14.0	8.0 -10.0	0.5 - 1.5	0.09 - 0.15	< 0.1	0.001-0.004

S. Sgobba, et al., Fusion Eng. Des. (2013), http://dx.doi.org/10.1016/j.fusengdes.2013.05.002
S. Sgobba et al., IEEE Transactions on Applied Superconductivity, **22**, 2012, p. 7800104

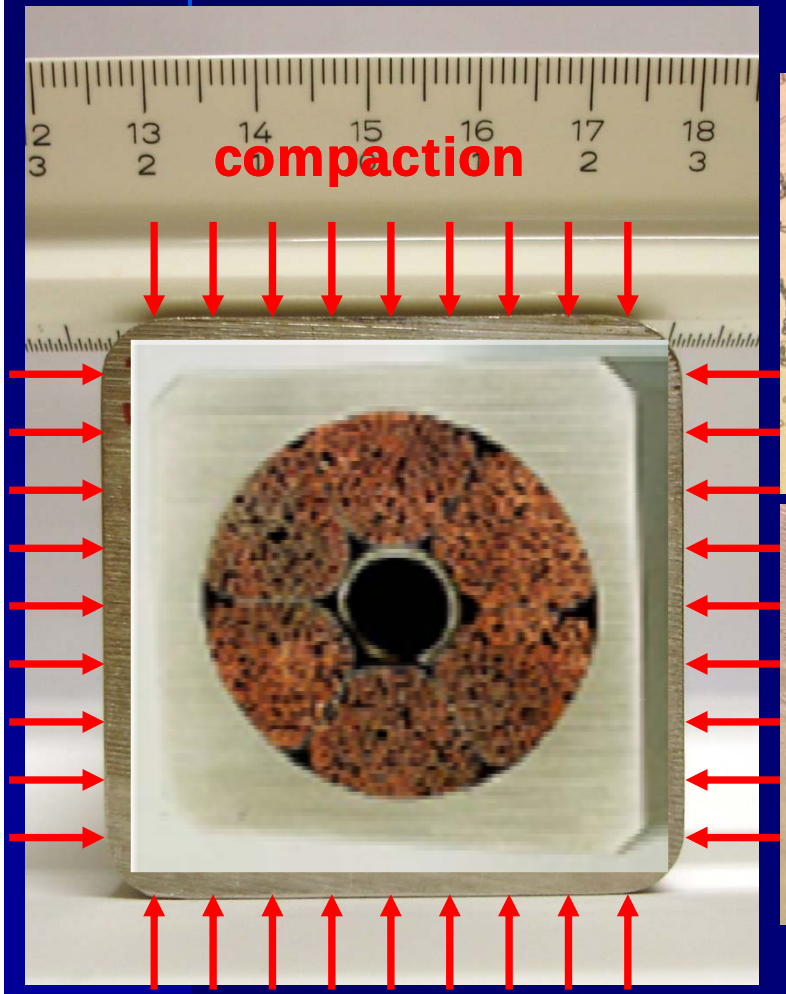

after aging, sensitization

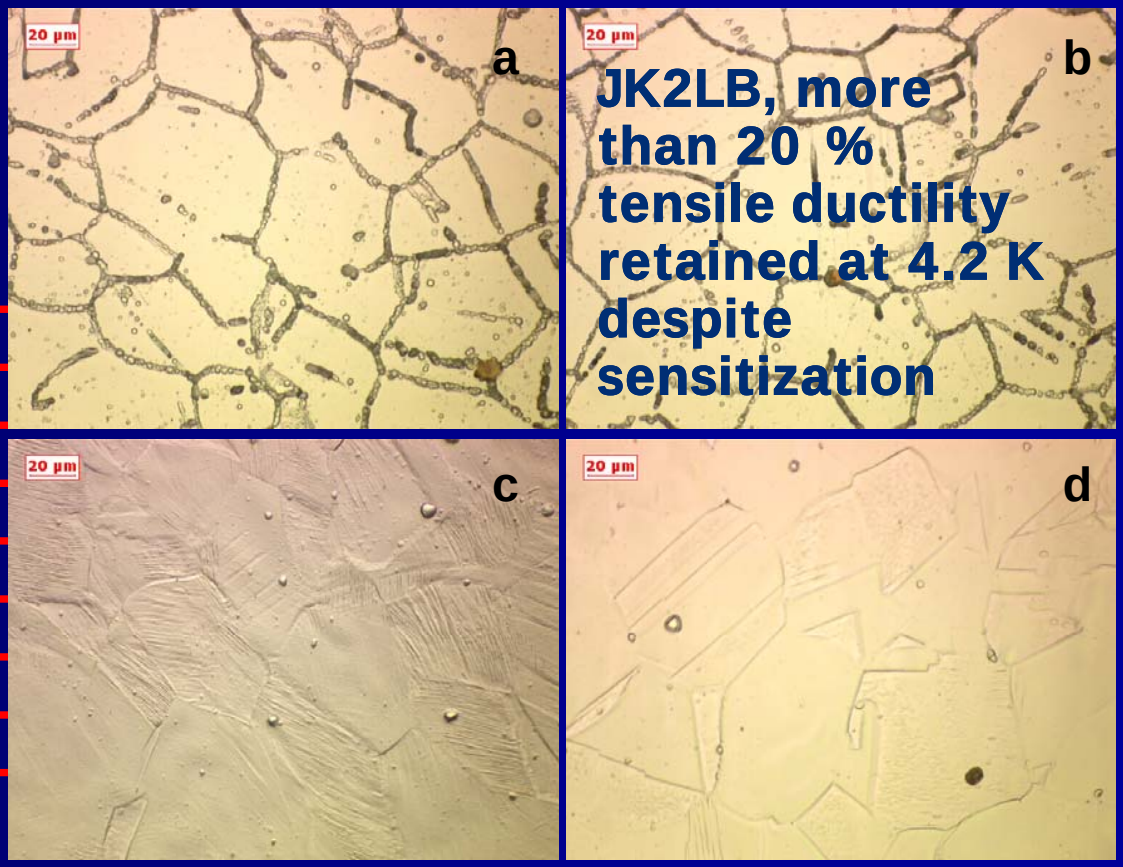

reference, before aging

followed by aging 650 °C – 200 h

Selection and characterization of structural materials for fusion magnets

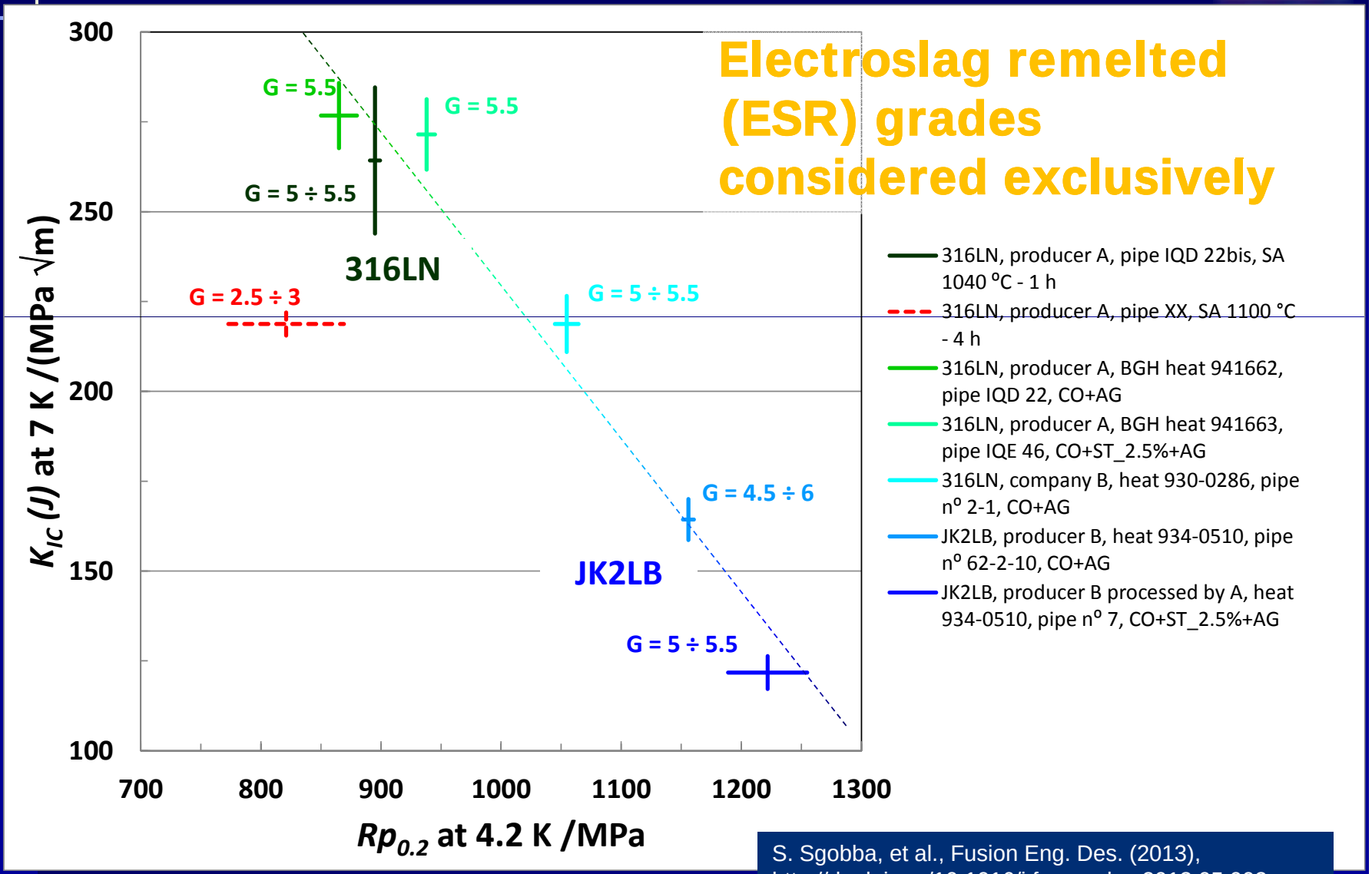

S. Sgobba, et al., Fusion Eng. Des. (2013), http://dx.doi.org/10.1016/j.fusengdes.2013.05.002

Selection and characterization of structural materials for fusion magnets:
TF He-inlet developments

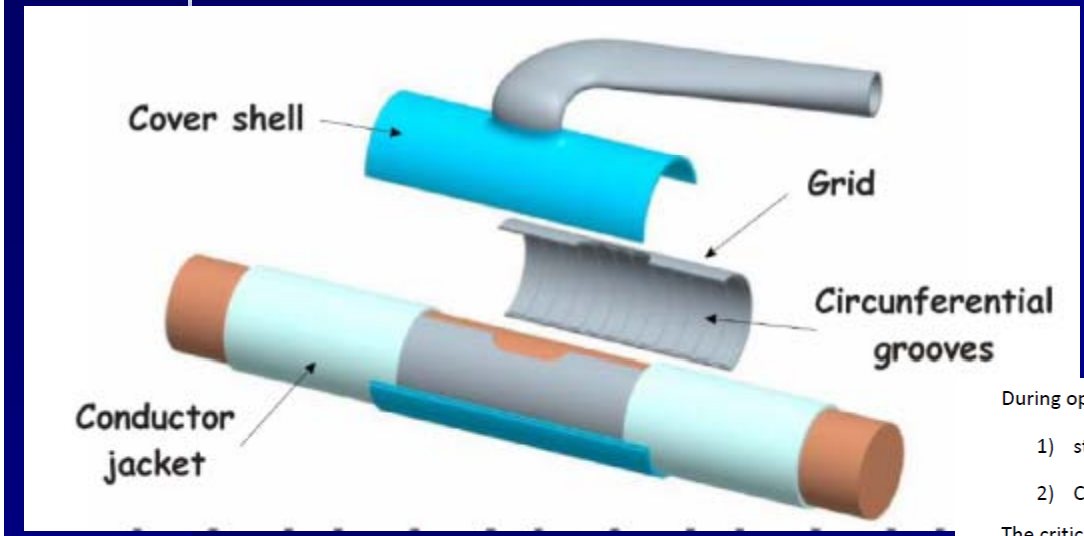

Fig. 3. TF-IN4 mock-up before test (lef

During operation, it will be submitted to

1) static loads (translated into strain of the order of 12×10^{-4})

2) Cyclic loads (translated into strain of the order of $+/- 2.3 \times 10^{-4}$)

The critical part of this inlet is the filet weld that joins the cover shell to the conductor jacket. There is a stress concentration at the toe of the filet weld that makes it critical from a fatigue point of view.

The picture shows what happened during a fatigue test carried out at FzK in 2005.

Breakdown after 476117 cycles, test under stress control, local stresses up to 550 MPa

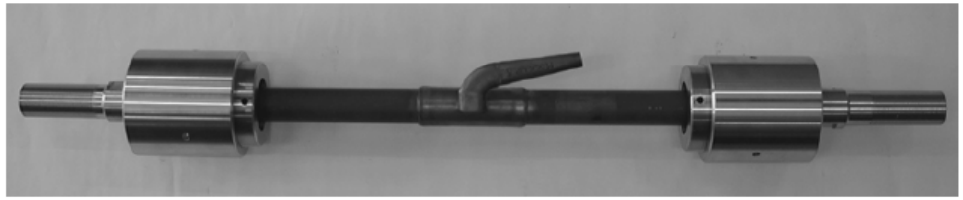

876 IEEE TRANSACTIONS ON APPLIED SUPERCONDUCTIVITY, VOL. 16, NO. 2, JUNE 2006

Design and Qualification of ITER CS and TF Cooling Inlets

P. Decool, H. Cloez, S. Nicollet, A. Nyilas, and J. P. Serries

TF He-inlet developments, weld qualification and effects of sensitization

Tensile test at RT and 4.2K, 316 LN welds with different weld schedules

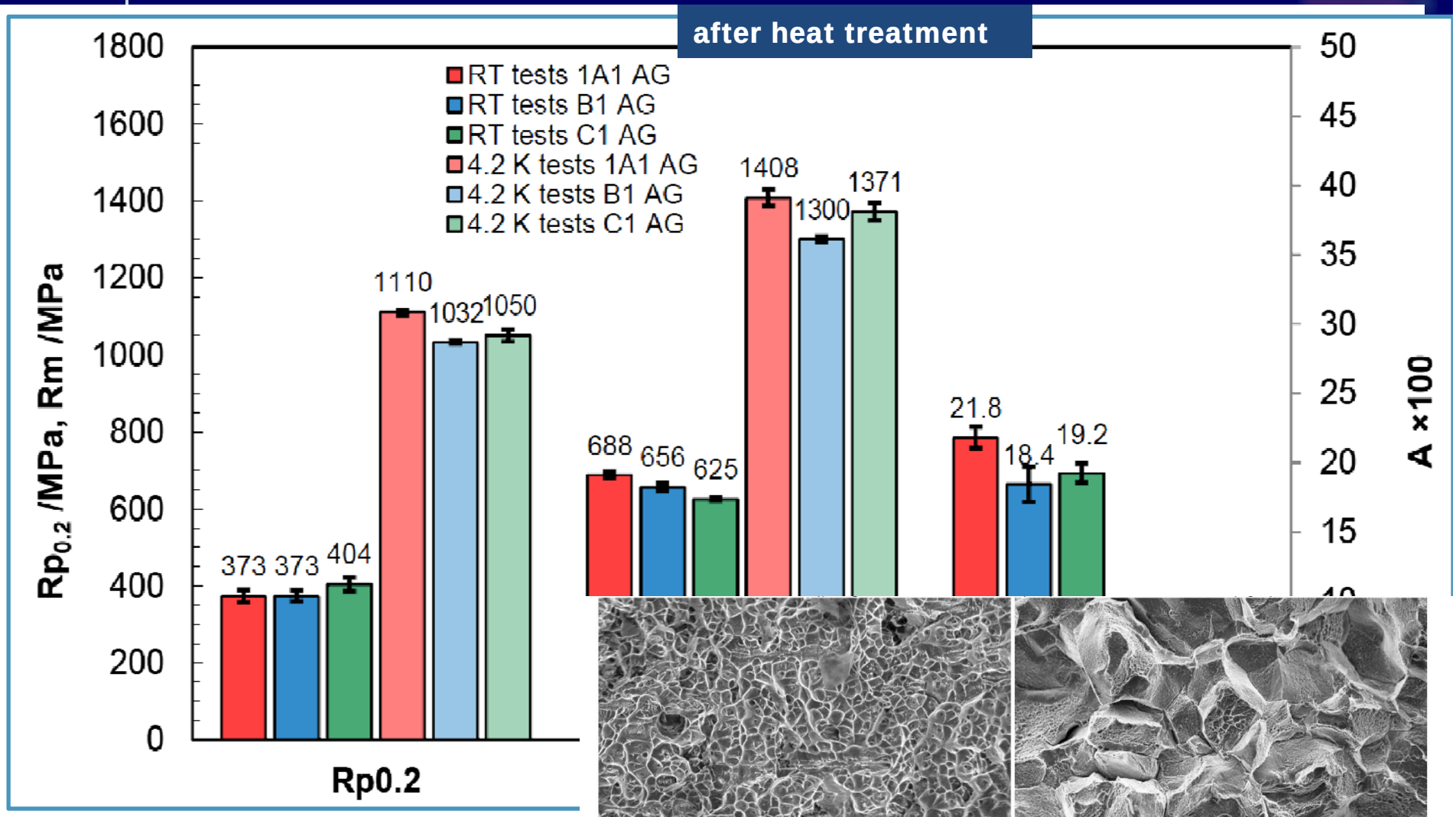

Figure 18: SEM on specimen without filler material (C1_C6 and C1_C12) after tensile test at 4.2K, magnification 400x: before (left, fracture in the weld bead) and after heat treatment (right, fracture between HAZ and the weld bead).

CERN EDMS report n° 1193170, 1208068

Selection and characterization of structural materials for fusion magnets:
additional He-inlet studies, ITER CC

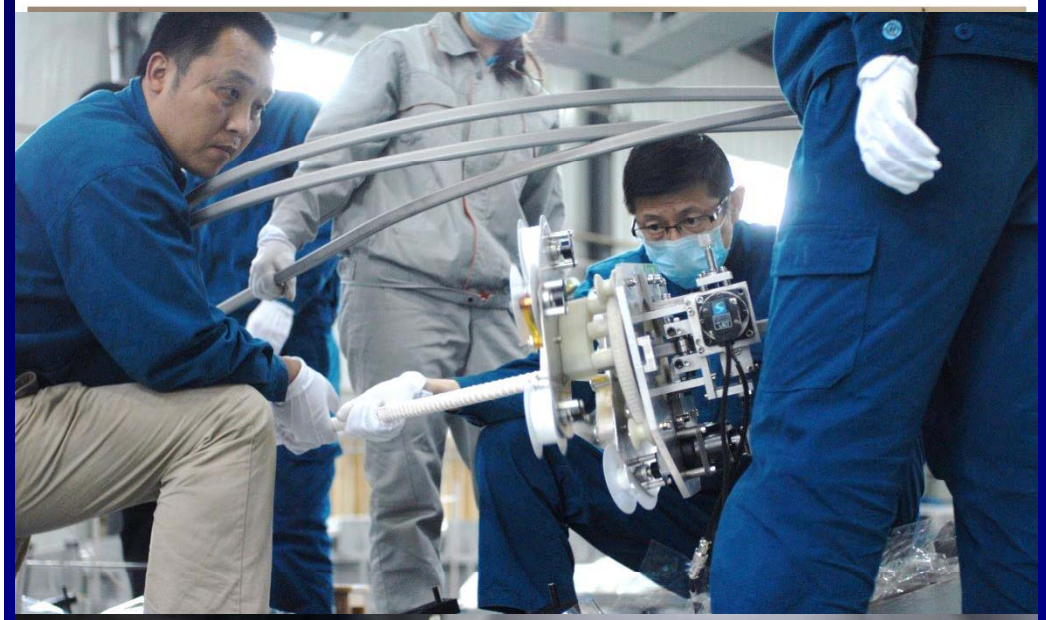

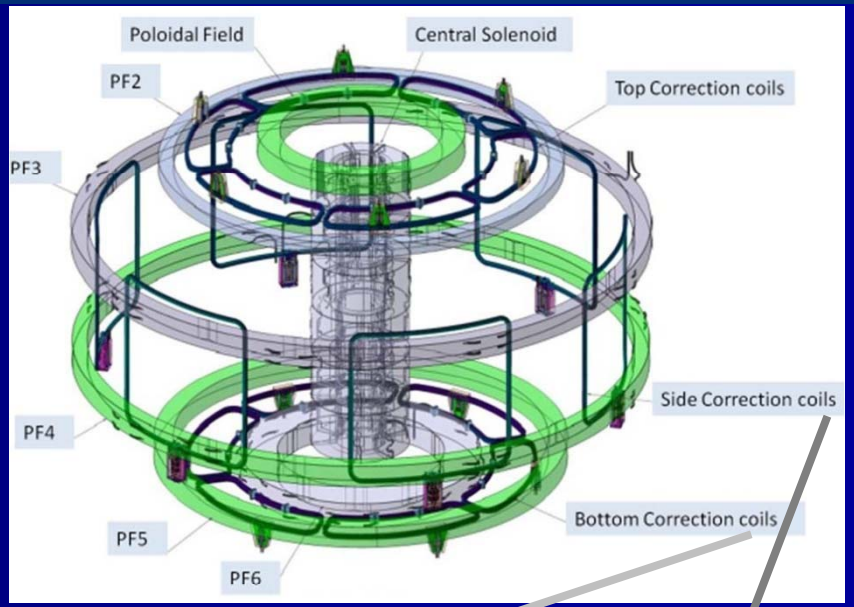

BCC /TCC

SCC

Selection and characterization of structural materials for fusion magnets:
additional He-inlet studies, ITER CC

- Laminography (planar tomography) by RX Solutions / FR
- Classification following ISO 6520-1 and judged with respect to EN ISO 5817 - level B

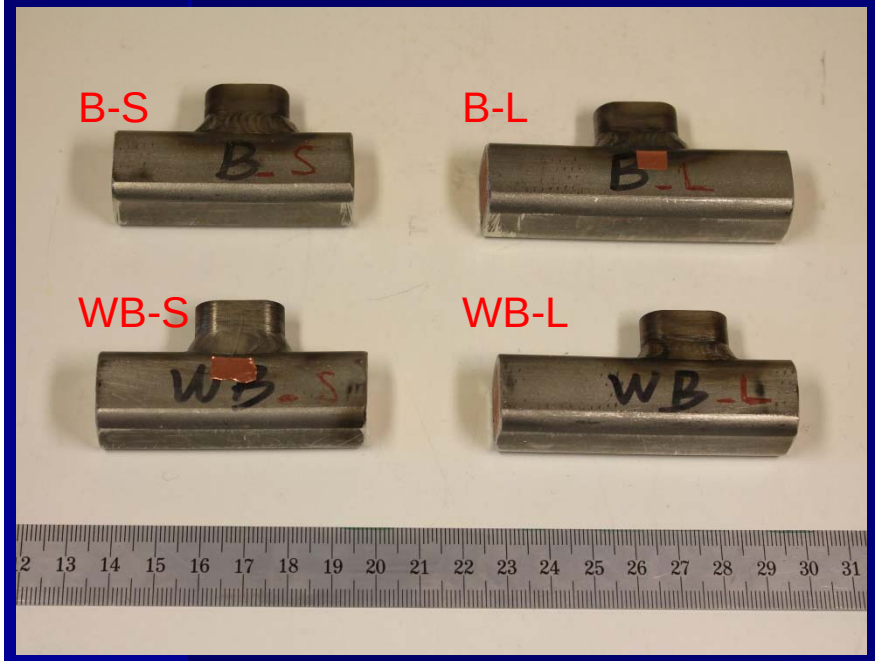

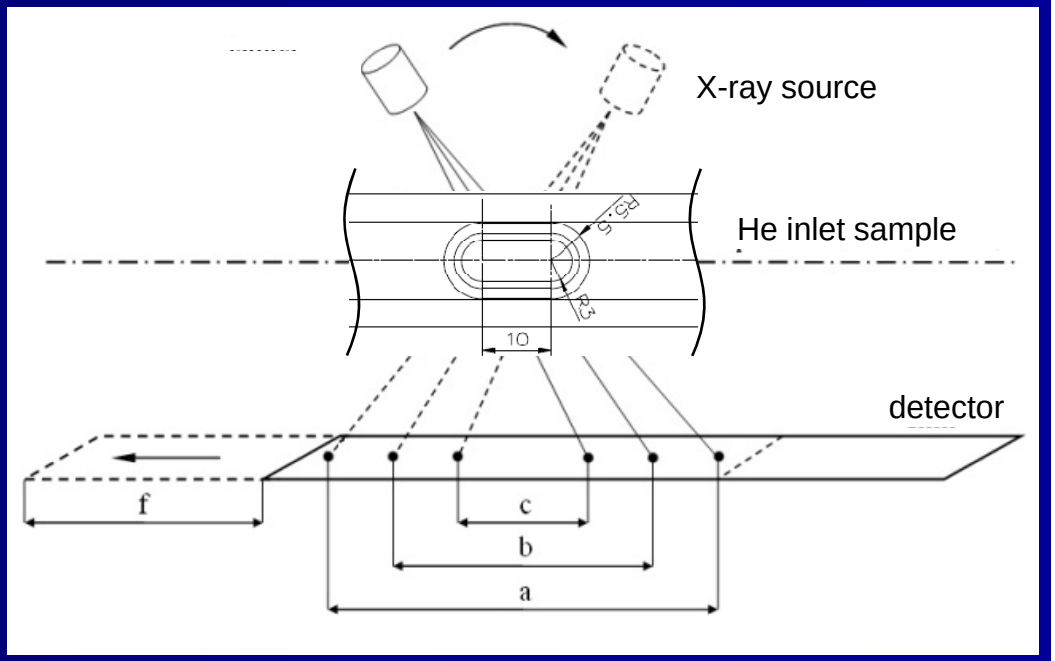

Selection and characterization of structural materials for fusion magnets:
additional He-inlet studies, ITER CC

Laminography weld WB-S

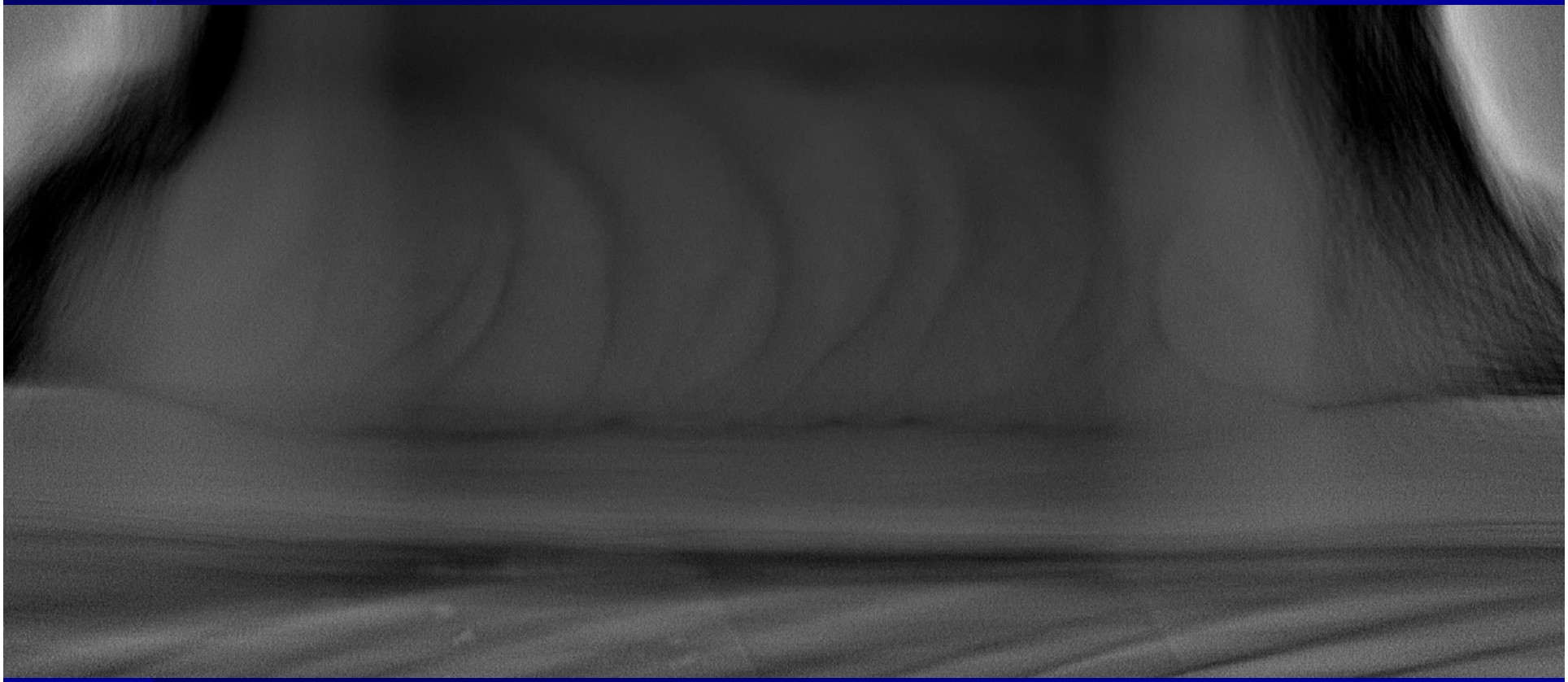

Selection and characterization of structural materials for fusion magnets: additional He-inlet studies, ITER CC

Laminography weld WB-S

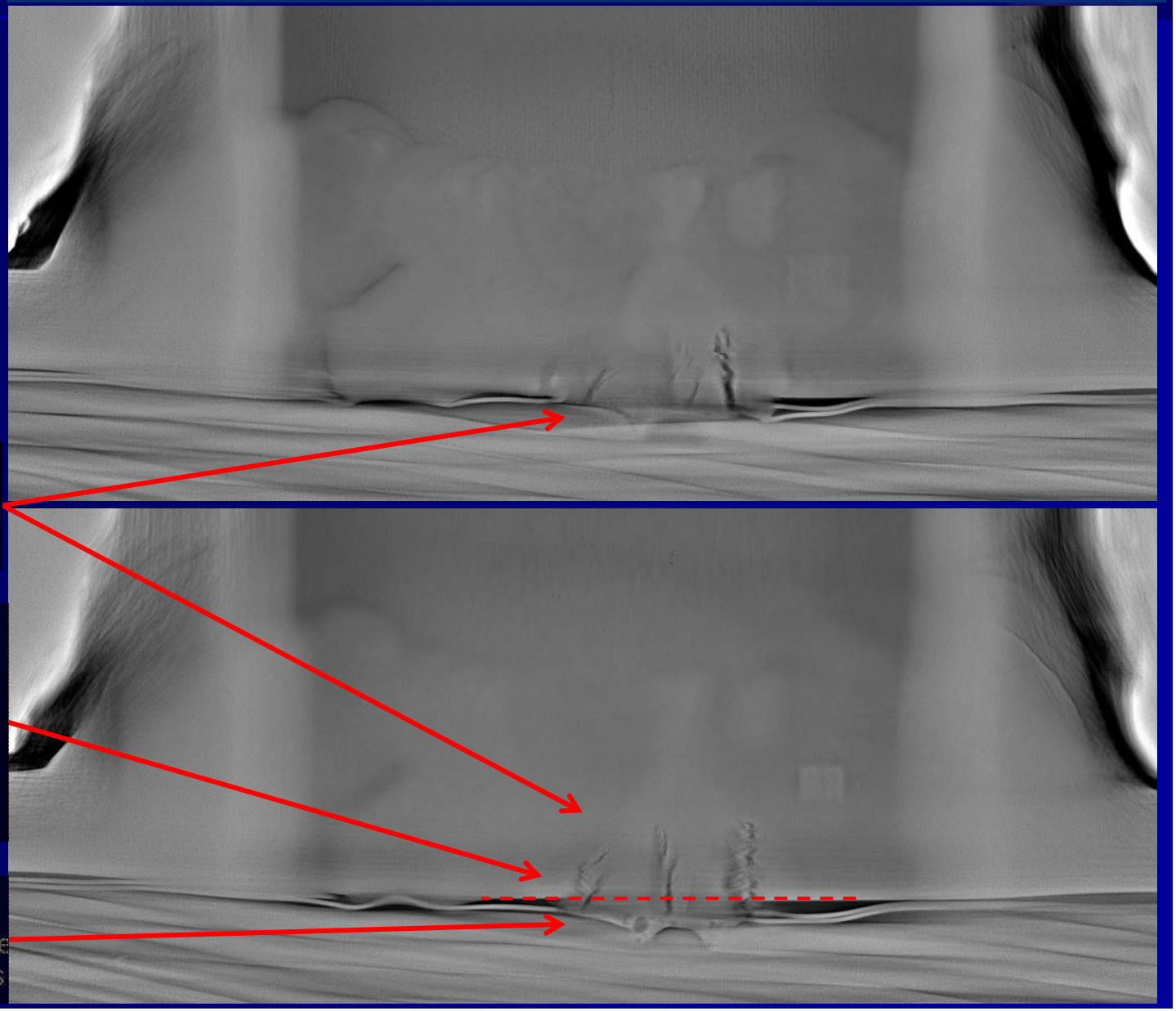

Cracks (ref: 401) unacceptable to ISO 5817 level B

Excessive penetration and melt through (ref: 504) acceptable to ISO 5817 level B ($h \leq 1\ mm + 0.1\ b$, where b is a width of weld reinforcement)

Wrap welded with the jacket and possibly with the superconductor

Selection and characterization of structural materials for fusion magnets: additional He-inlet studies, ITER CC

Laminography weld WB-S

Tungsten inclusion (ref: 6021) according to ISO 5817 level B acceptance depends on application

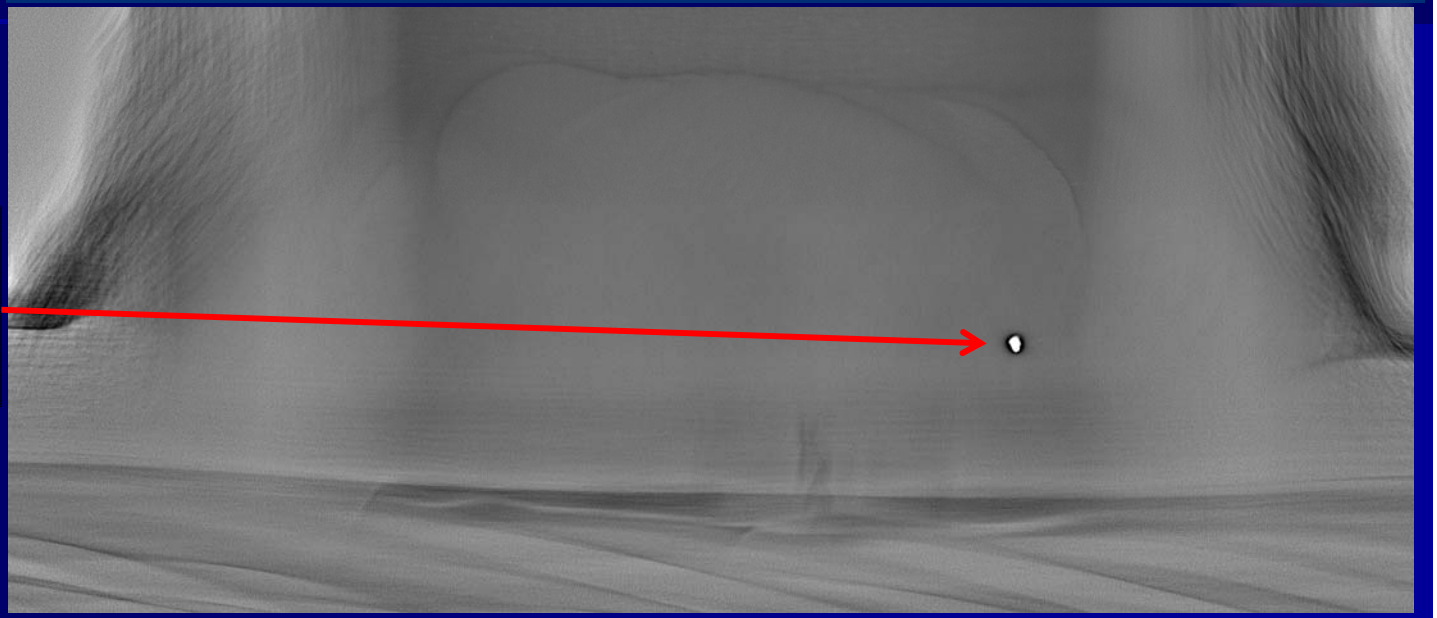

Shrinkage grooves (ref: 5013) not acceptable to ISO 5817 level B

Excessive penetration (ref: 504) acceptable to ISO 5817 level B ($h \leq 1\ mm + 0.1\ b$, where b is the width of weld reinforcement)

Laminography: impressive correspondence between XR tomography and microoptical observations

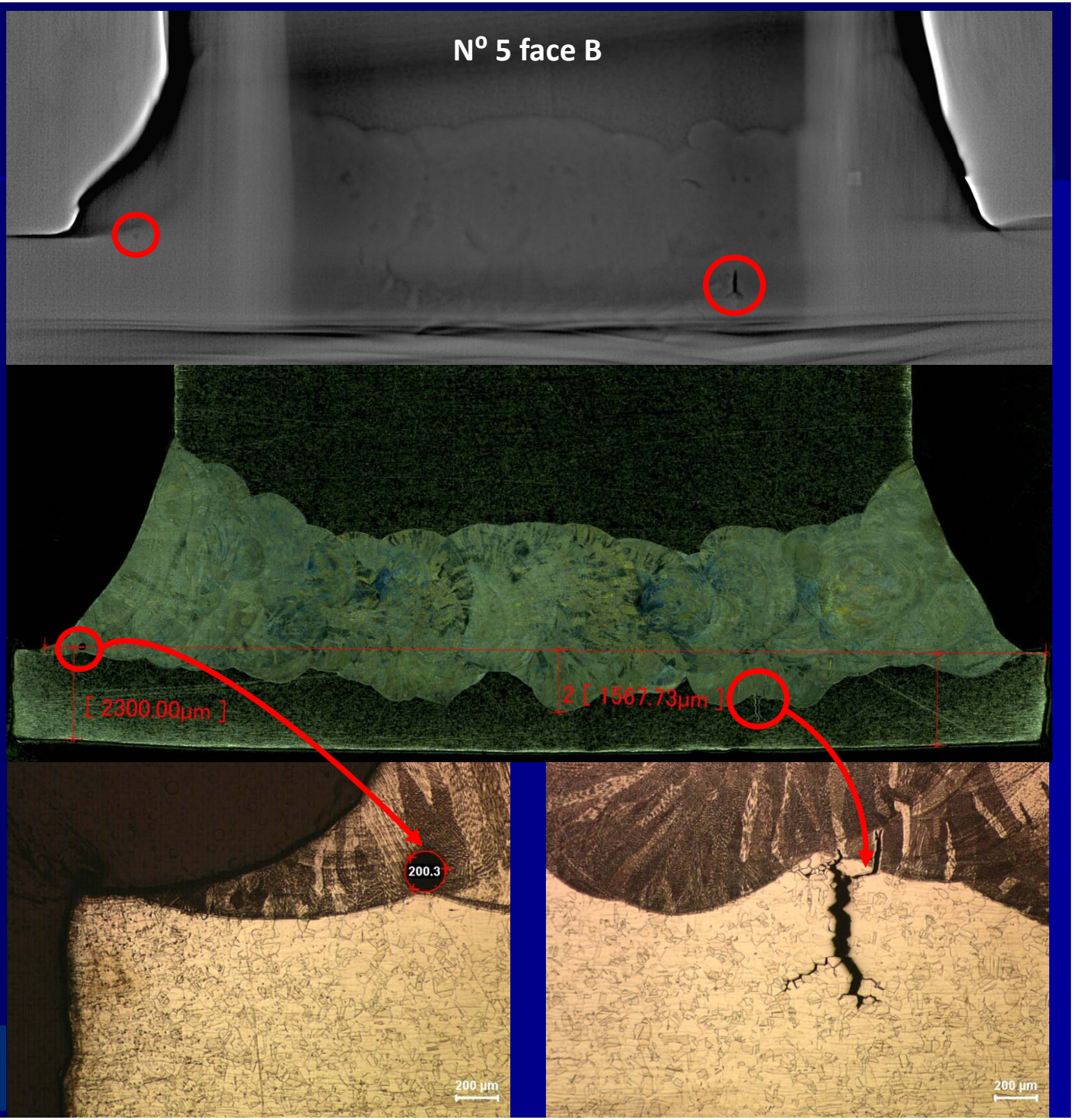

CERN report EDMS n° 1244255

Conclusions

- A structural material for a cryogenic application is not a mere "chemical composition" or a designation

Stainless steels

- 304L, general purpose ⇒ 7 $/kg
- 304L, vacuum/cryogenic application ⇒ 15 $/kg
- 316LN, as above ⇒ 20 $/kg
- 316LN, blanks ⇒ 60 (up to 150) $/kg
- P506, 316L convolutions for bellows ⇒ 50-100 $/kg

Al alloys

- plates EN AW 1050 ⇒ 6 $/kg
- special forgings ⇒ 30-35 $/kg
- 5N pure Al ⇒ 100 $/kg (medium quantities)
- Al-0.1%Ni ⇒ 100 $/kg (depends on quantities)

- Material selection (and procurement) to be operated at the beginning of a project


SIMBA
CEINTURES BRETELLES *
* belts, braces

Notes for "Selection and Properties of Structural Materials for Cryogenic Applications" - Stefano Sgobba

Slide 1-2	Structural materials play a crucial role in large cryogenic systems such as particle accelerators and experiments and their superconducting magnet systems. Adequate mechanical (strength, ductility, toughness), physical, magnetic and vacuum properties over the whole operating temperature range are important factors, either separately or in combination. Machinability, weldability or brazeability are also key parameters. The successful selection of a structural material for a cryogenic application is therefore closely related to obtaining a controlled microstructure and stable properties in service through the specification of a suitable manufacturing process.
Slide 3	Size of accelerators, hence materials quantities involved, has significantly increased with time. A picture of the 600 MeV CERN Synchrocyclotron, built in 1957 is shown that was CERN's first accelerator. It provided beams for CERN's first experiments in particle and nuclear physics.
Slide 4	The increasing size of CERN accelerators, until the Large Hadron Collider (LHC), the world's largest and most powerful particle accelerator consisting of a 27-kilometre ring of superconducting magnets including 1232 dipole magnets 15 meters in length working at 1.9 K, imposes severe constraints in terms of definition, specification and procurement of cryogenic structural materials. A large experience in selection and characterization of properties of structural materials for cryogenic applications has been gained during the construction of the LHC at CERN.
Slide 5	Stainless steel plays a crucial role in the construction of modern accelerators. The example of the dipole and quadrupole magnets of LHC is representative in this respect. A special high Mn austenitic stainless steel has been developed for the beam screen and the cooling capillaries of the machine vacuum system, retaining high strength, ductility and low magnetic susceptibility in the working temperature range between 10 K and 20 K. Several tens of kilometers of components have been produced in this special stainless steel grade for a total produced quantity of some 100 t. The magnet cold bore is manufactured as a seamless 316 LN tube. 11000 t of a more conventional non-magnetic high Mn grade, 3 mm thick strips have been delivered in kind by Japan between 2000 and 2004 for the magnet collars.
Slide 6	316 LN is also the reference grade for the shrinking cylinder of the dipole magnets (2500 bent plates of 15.35 m of length, 10 mm thick for a total weight of approx. 3000 t) The plates were welded longitudinally by a special Surface Tension Transfer (STT) technique combined with traditional pulsed MIG welding. In addition, more than 2800 magnet end covers of complex shape, including several nozzles, have been fabricated starting from HIPed 316 LN powders and near net shaped into geometry close to the final form.
Slide 7	Between the magnets, some 1700 interconnections consist of several thousand of leak tight components to be integrated, mainly working at cryogenic temperature (1.9 K). Interconnection components are also mainly based on austenitic stainless steels. For the convolutions of the several thousands of bellows involved in the machine and working under cyclic load at 1.9 K, a special remelted 316 L grade has been selected showing an extremely low inclusion content and improved austenite stability at the working temperature. The grade is highly formable at Room Temperature (RT).
Slide 8	A "beam screen" shields the magnet cold bore (held at 1.9 K) from the synchrotron radiation emitted by the circulating proton beam, and the power dissipated by the beam image currents. The screen is cooled to 10 K - 20 K by gaseous He circulating in cooling capillaries attached to its external wall. It consists of a 1 mm thick, 15 m long perforated tube, flattened top and bottom. The internal surface of the screen is covered by a thin layer of highly conductive colaminated OFE Copper. The screen was continuously formed and longitudinally laser welded. Laser welding minimizes the recrystallization of the Cu layer and preserves its low residual resistivity. Due to the proximity of the circulating beam, the screen and the laser welds must be totally non-

	magnetic (maximum acceptable relative magnetic permeability μ_r = 1.005 at the working temperature). Millions of laser spot welds attach the cooling capillary to the external wall of the beam screen. No one of these welds is allowed to leak, otherwise gaseous He would leak into the vacuum system of the machine.
Slide 9	AISI 300-series steels have magnetic susceptibility (μ_r - 1) well in excess of the limit value ($5 \cdot 10^{-3}$) at cryogenic temperatures due to antiferromagnetic transitions (resulting in peaks in the susceptibility versus temperature curves) occurring at excessively low temperature. Commercial high N steel grades such as UNS 21904 with Mn contents between 4 % and 9%, Ni between 7 % and 10%, N between 0.25 % and 0.38 % and C between 0.03 % and 0.11 % were first considered at CERN to replace AISI 300 steels for such non-magnetic applications. These steels generally show low μ_r, high mechanical properties and toughness. Their weldability is also excellent, both by conventional (TIG), or by electron and laser beam techniques. Nevertheless, independent of the choice of shielding gas and welding parameters, precipitation of δ-ferrite in laser welds cannot be avoided, bringing the magnetic permeability of the weld metal above the acceptable limit.
Slide 10	The new non-magnetic stainless steel specially developed for this application (P506) has an increased Mn content (12 %). The fully austenitic microstructure of the steel insures the non-magnetic behavior of the parent material; maintaining a high Ni content (11 %) compared to conventional grades allows in addition fully austenitic non-magnetic welds to be produced.
Slide 11	Laser welds of P506 are fully austenitic; a typical cellular dendritic structure develops in the weld bead. Independent of the choice of welding parameters, no tendency to hot cracking is observed. The extremely low residual content (P, S, B) obtained by selected ferroelements and ElectroSlag Remelting (ESR) prevents the susceptibility to hot cracking of the fully austenitic welds of this high purity P506 steel. On the contrary, hot cracking occurs as predicted in welds of austenitic grades featuring lower purity (e.g. steel P900).
Slide 12	The temperature of antiferromagnetic transition depends on composition. Increasing Mn content rises the temperature of antiferromagnetic transition. Higher temperature of antiferromagnetic transition allows for lower values of magnetic permeability at cryogenic temperature (see slide 9). On the other hand, antiferromagnetic transitions influence other physical properties such as the integral thermal contraction between RT and 4.2 K. The designed steel has an equilibrated composition and Mn not in excess of 12 % in order to avoid too high difference in thermal contraction with other components, generally manufactured in 316LN, that would have occurred if a very-high- Mn steel was selected.
Slide 13	As mentioned, the cold mass of the 1232 superconducting dipole magnets of LHC operating at 1.9 K is enclosed by a shrinking cylinder and two end covers at each extremity of the cylinder. The end covers are domed and equipped with a number of protruding nozzles for the passage of the different cryogenic lines. The covers are structural components that must retain high strength and toughness at cryogenic temperature. They are MIG welded onto the magnet shrinking cylinders. The protruding nozzles of the covers are welded to the interconnection pipes by an automatic orbital autogeneous TIG technique. Several thousand welds are present. AISI 316LN has been selected because of its mechanical properties, ductility, stability of the austenitic phase.
Slide 14	Due to the complex geometry of the end covers, a Powder Metallurgy (PM) + Hot Isostatic Pressing (HIPing) technique has been selected for the fabrication of the covers. PM is an attractive near-net-shaping technique, allowing the final shape to be

	approached and the machining to be reduced to a minimum. The covers have been produced from atomized powders of the relevant steel grade, blended, homogenized and filled into capsules with a geometry approaching the cover shape. After evacuation and sealing, a HIPing cycle has been performed. HIPing consists of a time-temperature-pressure cycle performed at 1180 °C during 3 h under a stress of 100 MPa, allowing a fully dense structure to be achieved. The capsulated covers have been solution annealed, water quenched, pickled to remove the capsules, ground and machined to the final dimensions. 100 % dye penetrant (PT), visual (VT) and ultrasonic (UT) inspection (to measure the wall thickness and detect possible volumetric defects) have finally been performed on the finished covers, showing no relevant defects and full soundness and compactness of the components. Closed or open die forging would require significantly more machining, a welded product would need extensive inspections and stress relieving, whilst a cast solution would feature poorer mechanical properties.
Slide 15	An extremely fine microstructure is featured by the PM covers (typical ASTM E112 grain size number is 6 to 7), much finer even than open die forged products (shown for comparison) and of cast + HIPed products that only show two grains in the whole thickness (also shown).
Slide 16	The chemical composition of the supplied covers is reported, showing exceptionally low oxygen content compared to PM austenitic stainless steel grades available in the past years.
Slide 17-18	Values of impact energy were evaluated at 4.2 K across a MAG weld between a 316LN wrought plate (W) and the PM cover. This absorbed energy is a measure of the impact strength of the material. BM stands for Base Metal, HAZ for Heat Affected Zone, WM for Weld Metal. Impact energies of PM products at 4.2 K are substantially lower than for wrought products. For each position, a series of three V-notch test pieces was measured as required by standards in force (individual measurement results are reported). SEM observations of impact fractures of the PM base metal show the typical presence of μm-size oxide inclusions within dimples. Nevertheless, the average impact energy value of 118 J (i.e. 153 J/cm^2) measured by us at 4.2 K for the PM base metal is much higher than the value reported by Couturier et al. for a PM 316LN with 200 ppm oxygen who measured at 77 K an impact energy under 100 J/cm^2. This high impact strength, compared to other PM products of the same grade, can be interpreted in terms of the low oxide inclusion content. The 316LN of the present study is produced with an oxygen content of only 110 ppm. The application of a standard PM product with higher oxygen content would have not allowed the required minimum impact energy to be reached.
Slide 19	PM was demonstrated as a technique fully adapted to the fabrication of complex shape components such as LHC end covers, working in a severe cryogenic environment and which have to be leak tight to superfluid helium. This is demonstrated by the excellent behavior of dipole magnets equipped with PM covers, which have performed satisfactorily in the machine. This near-net shaping technique, finally retained for the series production, was also selected on the basis of its price competitiveness. This development received the Award of the American Society for Metals (ASM International, Finland). In addition, CERN received together with its industrial partners the Grand Prize (Powder Metallurgy Design Excellence Award), in the frame of the PM Part Competition at PowderMet 2007, the International Conference on Powder Metallurgy and Particulate Materials in Denver, Colorado for the development of the Powder HIP End Covers for the LHC Project.
Slide 20	The Compact Muon Solenoid (CMS) is one of the general-purpose detectors provided for the LHC project at CERN. The 4-T, 6-m free bore CMS solenoid, operating at 4.5 K, has been successfully tested, operated and mapped at CERN during the autumn of

	2006; R&D studies started in 1993 and the construction in 1997. CMS contains the largest and the most powerful superconducting solenoid magnet ever built in terms of stored energy.
Slide 21	The right picture shows a view of the CMS solenoid, in the surface hall at Point 5 of the LHC, before the magnetic test in the autumn of 2006.
Slide 22	When looking at the density of stored magnetic energy per unit of cold mass for several detector magnets, the main parameters of the CMS project were considered beyond what was thought possible, as the total stored magnetic energy reaches 2.6 GJ for a specific magnetic energy density exceeding 11 kJ/kg of cold mass (see A. Hervé, D. Campi, B. Curé, P. Fabbricatore, A. Gaddi, F. Kircher, and S. Sgobba, "*Experience Gained From the Construction, Test and Operation of the Large 4-T CMS Coil*", IEEE Transactions on Applied Superconductivity, Vol. 18, 2008). During this period several important technical choices were made, including selection of advanced materials and processes, to maximize the chances of reaching the nominal induction of 4 T.
Slide 23	The solenoid was manufactured as a layered (4-layers winding) and modular structure of NbTi cables embedded in a high purity (99.998%) Al-stabilizer. Each layer consists of a wound continuous length of 2.55 km within an Al-alloy external cylinder.
Slide 24	In order to withstand the high electromagnetic forces, two external aluminum alloy reinforcing sections were foreseen. These reinforcements, of 24 mm × 18 mm cross-section, were continuously electron beam (EB) welded to the pure Al-stabilizer. The alloy EN AW-6082 was selected for the reinforcements due to its excellent extrudability, high strength in the precipitation hardened state, high toughness and strength at cryogenic temperatures and ready EB weldability.
Slide 25	An improved billet on billet extrusion process of continuous aluminum alloy shapes had to be developed for the CMS conductor. Each one of the 2.55 km continuous sections of reinforcement is extruded billet on billet and press quenched on-line from the extrusion temperature in an industrial extrusion plant.
Slide 26	The region where billet on billet welds develop is usually defective and represents a discontinuity in the extruded product, where improper quenching conditions associated to the stop of the line induce poorer mechanical properties. For the application to CMS, thanks to an optimization of the process, almost isothermal extrusion could be achieved, despite the discontinuous process. This, associated to a proper conditioning of the mating surface of the billet, allowed the local degradation of the yield strength to be minimized. The achievement of homogeneous strength along continuously extruded long shapes, which was important for the CMS coil winding, might also be crucial for structural applications where homogeneity of properties has to be maintained over long lengths.
Slide 27	Since EN AW-6082 undergoes natural ageing and in order to avoid dispersion of the mechanical properties, an artificial ageing treatment (underageing) was applied on the coiled sections. The temper associated with this fabrication method is referred as T51 Underageing was specified as an artificial ageing aimed at achieving after the curing cycle a further overall increase of the tensile yield strength. The underaged temper has the advantage of allowing peak-aged properties (T6) to be achieved only after the curing cycle applied on the wound magnet. The relatively low tensile properties in the as-received state facilitated spooling and despooling of the reinforcement coils, necessary for the EB operation, and coil winding.
Slide 28	In view of an upgrade of the CMS conductor oriented to a possible new project, an improvement of the mechanical performances of the reinforced conductor starting from the CMS concept was considered, aimed at increasing the achievable field based on an optimized layout. This improvement might be obtained by the replacement of the pure Al stabilizer by a cold drawn Al-0.1 wt%Ni alloy, first developed for the ATLAS thin solenoid superconductor, allowing mechanical strength to be enhanced without

	excessive degradation in RRR compared to pure Al. The replacement of the reinforcement alloy EN AW-6082 by a higher strength alloy EN AW-7020 (Al-Zn4.5Mg1) was also initially studied. This extrudable and weldable alloy (an example of a mixed EB weld with Al-0.1 wt%Ni is shown) maintains high ductility and strength at 4.2 K even after curing.
Slide 29	The present developments for the SiD Solenoid aim at a 5 T magnetic field in a 5.4 m bore diameter (~20 kA operating current). The present goal is to develop a prototype 5 T class stabilized superconductor, operating at 4.2 K for a 60 kA critical current. The development targets a conductor with a ~ 2000 mm^2 cross-sectional area. The stabilizer should feature a yield strength of >120 MPa at 4.2 K and a RRR above 500.
Slide 30	Al-0.1 wt%Ni alloy is considered for this development. Aluminum stabilized superconductors have been reinforced in the past years either by homogeneous reinforcement, thanks to diluted Al-alloys hardened by cold-working (including for experiments in space) better resistant against annealing than cold worked high purity aluminum, or by an hybrid configuration as applied to the CMS conductor. A challenge which is faced by present developments is to obtain large cross-section conductors stabilized by cold worked Al-0.1 wt%Ni with sufficient mechanical properties.
Slide 31-33	Almost all large indirectly cooled solenoids constructed to date (e.g., Zeus, Aleph, Delphi, Finuda, Babar) comprise Al-alloy mandrels fabricated by welding together plates bent to the correct radius. The external cylinder of CMS consists of five modules having an inner diameter of 6.8 m, a thickness of 50 mm and an individual length of 2.5 m. It has been manufactured by bending and welding thick plates (75 mm) of the strain hardened aluminum alloy EN AW-5083-H321. The required high geometrical tolerances and mechanical strength (a yield strength of 209 MPa at 4.2 K) imposed a critical appraisal of the design, the fabrication techniques, the welding procedures and the quality controls. In particular the thick flanges at both ends of each module have been fabricated as seamless rolled rings, circumferentially welded to the body of the modules. Ring rolling is a metalforming process allowing seamless annular components to be obtained starting from a pierced, pre-formed and pre-heated blank. The use of a computer controlled, multiple mandrel, radial-axial ring mill (the largest in Europe) allowed rings of high planarity and circularity tolerances to be obtained. A relationship between radial and axial cross-sectional reduction is selected, controlling the diameter growth rate during the rolling. Rolling is followed by a final cold expansion (performed in an expander), aimed to calibrate the ring and, in our case, to confer the adequate mechanical properties to the ring by cold stretching. To our knowledge, the ring rolled Al-alloy flanges adopted for the CMS external cylinder are the largest seamless Al-alloy rings produced to date.
Slide 34	Since several years CERN is involved in a co-operation with ITER to support material studies, by providing testing and consultancy for the construction of the ITER Magnet System. The magnet system of ITER comprises 18 Toroidal Field (TF) coils, a Central Solenoid (CS), 6 Poloidal Field (PF) coils and 18 Correction Coils (CCs). All coils are superconducting: Nb_3Sn conductors form the core of the CS and the TF while the PF and the CC coils are manufactured from NbTi.
Slide 35	The ITER Central Solenoid (CS) includes six identical coils called modules, using a cable-in conduit conductor, stacked upon each other and surrounded by a vertical precompression structure. When energized, these coils experience large electromagnetic forces. If the net resulting loads are transferred to the TF coils through a support structure, the internal loads have to be resisted by the coils themselves. Whereas the radial forces transfer into a tensile hoop load in the toroidal direction, the vertical forces apply a vertical compression to the coils. These loads, combining

	longitudinal tension with transverse compression are resisted by the conductor jacket itself, which is the main structural element of the CS coils. As plasma operation is pulsed, the design is driven by fatigue behavior (60 000 cycles) of the CS conductor jacket. The availability of a suitable conductor jacket material is thus a key point to achieve safe operation of the CS. This led to the early procurement of a small production of CS conductor jackets to address as well the setting up of industrial production including NDT procedures and mechanical characterization of the produced jackets.
Slide 36	The conductor jacket of the ITER CS consists of circle-in-square extruded and drawn austenitic stainless steel pipes. One particular aspect is the heat treatment of the wound conductor to form the Nb_3Sn, to be carried out at 600°C for a duration of around 200 h, the impact of which on the mechanical performances had to be verified. Two materials have been considered: a special high manganese austenitic stainless steel, developed in Japan and called JK2LB (the grade finally retained), and a modified 316LN stainless steel with very low carbon content to prevent sensitization. The high Mn-bearing austenitic stainless steel JK2LB features tensile yield strength $Rp_{0.2}$ above 1000 MPa at 4 K, well above the minimum yield strength of 719 MPa imposed to the jacket material at 4 K. This grade must provide minimum specified fracture toughness K_{IC} *(J)* of 130 MPa√m following the mentioned superconductor reaction aging treatment. JK2LB has been selected as jacket material also because of its lower coefficient of thermal expansion between RT and 4 K, compared to conventional AISI 300-series steels such as 316LN (see slide 12), allowing for an additional precompression of the CS modules during cooling down. An extensive qualification of the production of stainless steel jacket material arising from two different suppliers was carried out on jackets manufactured in both a modified 316LN with extra-low carbon (0.015 %) and JK2LB. Manufacturing by forging of a prototype tie-plate for the CS vertical precompression structure, obtained as a single seamless piece, is also discussed.
Slide 37	A Phased Array Ultrasonic Testing (PAUT) sectorial scan inspection method was developed to examine almost 95 % of the volume of the jackets, despite their complex geometry.
Slide 38	After the aging treatment following compaction, or compaction and stretching, some sensitization has been previously observed at grain boundaries (GB) of 316LN jackets in the form of discontinuous $M_{23}C_6$ precipitation at the initial stage of development, partially surrounding the austenite grains. Sensitization effects occur as well on JK2LB grade following the same treatments. Optical observations confirm sensitization on compacted and compacted + strained samples after aging. Sensitization is confirmed by the presence of ditches at GB. GB precipitation is expected for the applied aging treatment, carried out in a critical temperature and time range. As expected, non-aged samples show unsensitized step structure free of ditches. Nevertheless, more than 20 % tensile ductility is retained by JK2LB at 4.2 K despite sensitization.
Slide 39	For the two grades, particular attention has been paid during development to ensure refined and clean steel microstructures featuring a limited amount of non-metallic inclusions and an absence of exogenous macro-inclusions, by including an Electroslag Remelting (ESR) in the steelmaking process. The results of low temperature K_{IC} *(J)* measurements are plotted as a function of $Rp_{0.2}$ for different series of JK2LB and, for comparison, 316LN jackets. Fine grain size (ASTM grain size numbers, reported in the plot, above 4) provides higher strength and fracture toughness. Despite the different chemical analysis, product origin and metallurgical states, all fine grained JK2LB and 316LN series follow the same trend of dependence of K_{IC} *(J)* on $Rp_{0.2}$. For JK2LB series featuring lower yield strength, the minimum specified value of 130 MPa√m could be achieved.

Notes for "Selection and Properties of Structural Materials for Cryogenic Applications" - Stefano Sgobba

Slide 40	Sensitization phenomena may also be critical for the TF jackets and their welds, e.g. the fillet welds of the He inlets. A fatigue test at 4 K carried out in 2005 ended with premature rupture.
Slide 41	In order to qualify the intrinsic effects of sensitization, in the frame of TF He-inlet developments dedicated tensile and fatigue test campaigns at cryogenic temperature have been carried out on low C, 316LN standard weld plates obtained with three different weld schedules (1A1: JK2LB filler, ∅ 1.6 mm; B1: 1.4453 filler, ∅ 1.2 mm; C1: with no filler). Elongation at breakdown of weld joint under 10 % at 4.2 K results from the reaction heat treatment. The mode of rupture changes from ductile to quasi-cleavage due to sensitization.
Slide 42	Additional He-inlet studies have been carried out for ITER CC magnets. CC are developed to reduce the magnetic error fields created by imperfections in the location and geometry of the other coils used to confine, heat, and shape the plasma. The system consists of three sets of 6 coils each, located at the top (TCC), side (SCC) and bottom (BCC) of the Tokamak device and using a NbTi cable-in-conduit supercon-ducting conductor. In this case, sensitization is not an issue (NbTi conductor), but the soundness of the fillet weld between the inlet and the jacket has to been guaranteed.
Slide 43	The whole volume of He-inlet welds is virtually uninspectable by conventional NDT techniques, and in particular by conventional radiography. X-Ray Computed Tomography (CT) is a NDT technique that is successfully applied to inspect the full weld volume of qualification weld inlet samples.
Slide 44	CT requires a relative movement of the X-ray source and the detector with respect to the sample to be inspected. For these welds, the technique is applied in laminographic “shear” mode, allowing a layer-wise imaging with X-rays by a coordinated movement of source and detector in opposite directions. Laminographic inspections allow exploring, layer after layer following image reconstruction, the whole volume of the welds.
Slide 45-46	Weld imperfections can be easily imaged and their position can be assessed in the volume. Defects can be quantified and assessed according to standards in force.
Slide 47	An impressive one-to-one correspondence between X-Ray tomography (virtual cuts allowing very small defects to be identified in the volume) and micro-optical observations, confirming the same defects in the same positions, is demonstrated.
Slide 48	The conclusions insist on the importance of the selection of structural materials for cryogenic applications, that should be made at an early stage of a project, taking into account also budget implications (the unit price could be increased by a factor over ten between a material available from the shelf and a material specially produced with targeted requirements and controls).
Slide 49	An adequate material specification and selection of manufacturing process can allow cost savings (e.g. powder metallurgy solution for the LHC magnet end covers), while avoiding over-specifying. It is better to be safe than sorry, but belt and braces approach is not always applicable!